

Electronic structure and carrier transfer in B-DNA monomer polymers and dimer polymers: Stationary and time-dependent aspects of wire model vs. extended ladder model

K. Lambropoulos,¹ M. Chatzieftheriou,^{1,*} A. Morphis,¹ K. Kaklamanis,¹
R.Lopp,^{1,†} M. Theodorakou,¹ M. Tassi,¹ and C. Simserides^{1,‡}

¹*National and Kapodistrian University of Athens, Faculty of Physics,
Panepistimiopolis, 15784 Zografos, Athens, Greece*

(Dated: September 2, 2016)

We employ two Tight-Binding (TB) approaches to study the electronic structure and hole or electron transfer in B-DNA monomer polymers and dimer polymers made up of N monomers (base pairs): (I) at the base-pair level, using the on-site energies of base pairs and the hopping integrals between successive base pairs, i.e., a wire model and (II) at the single-base level, using the on-site energies of the bases and the hopping integrals between neighboring bases, i.e., an *extended* ladder model since we also include diagonal hoppings. We solve a system of MD (“matrix dimension”) coupled equations [(I) $MD = N$, (II) $MD = 2N$] for the time-independent problem, and a system of MD coupled 1st order differential equations for the time-dependent problem. We study the HOMO and the LUMO eigenspectra, the occupation probabilities, the Density of States (DOS) and the HOMO-LUMO gap as well as the mean over time probabilities to find the carrier at each site [(I) base pair or (II) base], the Fourier spectra, which reflect the frequency content of charge transfer (CT) and the pure mean transfer rates from a certain site to another. The two TB approaches give coherent, complementary aspects of electronic properties and charge transfer in B-DNA monomer polymers and dimer polymers.

PACS numbers: 87.14.gk, 82.39.Jn, 73.63.-b

I. INTRODUCTION

Today, remarkable parts of the physical, chemical, biological and medical communities as well as a broad spectrum of other scientists and engineers is interested in charge transfer (CT) in biological systems. CT is the basis of many biological processes e.g. in various proteins¹ including metalloproteins² and enzymes³, with medical and bioengineering applications^{4,5}. CT plays a central role in DNA damage and repair⁶⁻⁸. CT might also be an indicator to discriminate between pathogenic and non-pathogenic mutations at an early stage⁹.

DNA plays a key role in the development, function and reproduction of living organisms, because the sequence of its bases (adenine, guanine, thymine, cytosine) carries their genetic code, hence, its study is usually associated with molecular biology and genetics. However, its remarkable properties have spurred in recent years the interest of a broad interdisciplinary community. From the perspective of physics, its electronic structure and its CT properties are studied with the aim of understanding its biological functions as well as its potential applications in nanotechnology (e.g. nanosensors, nanocircuits, molecular wire).

At least for twenty years, we try to understand carrier movement through DNA¹⁰⁻¹⁶. Today, we know that many external factors related to the environment, like aqueousness and presence of counterions, extraction process, conduct quality with electrodes, purity, substrate and so on, influence carrier movement. This leads to the need of a deeper understanding of endogenous factors affecting carrier movement in DNA, like base-pair

sequence and geometry. Maybe the most important endogenous factor is the base-pair sequence, to which this article is devoted, too.

Additionally, we have to discriminate between the words *transport* (usually implying the use of electrodes), *transfer*, and *migration* (a transfer over rather long distances). The carriers (electrons or holes) can be either inserted via electrodes or generated by UV irradiation and by chemical reduction or oxidation. Moreover, although unbiased charge transfer in DNA nearly vanishes after 10 to 20 nm^{17,18}, DNA still remains a promising candidate as an electronic component in molecular electronics, e.g. as a short molecular wire¹⁹. Favoring geometries and base-pair sequences have still to be explored e.g. incorporation of sequences serving as molecular rectifiers, using non-natural bases or using the triplet acceptor anthraquinone for hole injection²⁰. Structural fluctuations could be another important factor which influences quantum transport through DNA molecular wires²¹. Finally, the carrier transfer rate through DNA can be manipulated by chemical modification²².

On theoretical side, both *ab initio* calculations²³⁻²⁹ and model Hamiltonians³⁰⁻³⁸ try to interpret the diversity of experimental results and ascertain the underlying CT mechanism. The former can provide a more detailed description, but are currently limited to very short segments, while the latter are much less detailed but allowing to address systems of realistic length, grasping hopefully the underlying physics³⁹. Here we study rather long B-DNA segments, hence we adopt the latter approach.

Specifically, we employ two Tight-Binding (TB) approaches. TB I is very simple, it is an approach at the

base-pair (bp) level. We need the on-site energies of base pairs and the hopping integrals between successive base pairs. In other words, TB I is a *wire* model⁴⁰. TB II is an approach at the single-base (sb) level. We need the on-site energies of bases and the hopping integrals between neighboring bases. We also include diagonal hoppings, in that sense, TB II is an *extended ladder* model³⁹. The inclusion of diagonal hoppings is crucial in some cases as will become evident below. With these two TB models we study the electronic structure and hole or electron transfer in B-DNA monomer polymers and dimer polymers. This means that we call *monomer* a B-DNA base pair and study polymers made of N monomers, with repetition unit one or two monomers. To this end, we shall see below, we have to solve a system of MD (“matrix dimension”) coupled equations for the time-independent problem, and a system of MD coupled 1st order differential equations for the time-dependent problem. In TB I $MD = N$, while in TB II $MD = 2N$. In this article, we study HOMO and LUMO eigenspectra and the relevant Density of States (DOS) as well as the mean over time probabilities to find the carrier at each site, which is a base pair for TB I and a base for TB II. We are also interested in the frequency content of carrier movements, hence, we analyze the Fourier spectra, too. The pure mean transfer rate from a certain site to another describes the easiness of CT; it gives us a measure of how much of the carrier is transferred and also of how fast this process is. Our two TB approaches give coherent, complementary aspects of electronic properties and charge transfer in these B-DNA monomer polymers and dimer polymers.

The rest of the paper is organized as follows: In Section II we delineate the basic theory behind the time-independent (Subsection II A) and the time-dependent (Subsection II B) problem. In Section III we discuss our results for eigenspectra and eigenvectors (Subsection III A), the density of states (Subsection III B), the HOMO-LUMO gaps (Subsection III C), the mean over time probabilities to find the carrier at each site (Subsection III D), the CT frequency content (Subsection III E), and the pure mean transfer rates (Subsection III F). In Section IV we state our conclusions.

II. THEORY

Let us begin with some notations. We call *monomer* a B-DNA base pair. We denote a system of two successive monomers by YX , according to the convention

$$\begin{array}{c|cc}
 & \sigma=1 & \sigma=2 \\
 \hline
 \vdots & 5' & 3' \\
 \mu & Y & - Y_{\text{compl}} \\
 \mu+1 & X & - X_{\text{compl}} \\
 \vdots & 3' & 5'
 \end{array} \quad (1)$$

for the B-DNA strands orientation. X_{compl} (Y_{compl}) is the complementary base of X (Y). The base pair $X-X_{\text{compl}}$ is separated and twisted by 3.4 \AA and 36° , respectively, relatively to the base pair $Y-Y_{\text{compl}}$, around the B-DNA growth axis. We call μ the monomer index, with $\mu = 1, 2, \dots, N$, and σ the strand index ($\sigma = 1$ for the strand with $5'-3'$ directionality, $\sigma = 2$ for the strand with $3'-5'$ directionality). Further, we define the base index $\beta(\mu, \sigma)$, $\beta = 1, 2, \dots, 2N$, according to the expression $\beta = 2(\mu - 1) + \sigma$. Schematically,

$$\begin{array}{c|c|c}
 \mu & \sigma & \beta \\
 \hline
 1 & 1 & 1 \\
 1 & 2 & 2 \\
 2 & 1 & 3 \\
 2 & 2 & 4 \\
 \vdots & \vdots & \vdots
 \end{array}$$

In this work, we study all possible periodic B-DNA segments of the form $YXYX\dots$, consisting of N monomers, i.e., monomer polymers and dimer polymers. There are three types of such polymers:

(type α') poly(dG)-poly(dC), poly(dA)-poly(dT),
 (type β') GCGC..., CGCG..., ATAT..., TATA..., and
 (type γ') ACAC..., CACA..., TCTC..., CTCT...,
 AGAG..., GAGA..., TGTG..., GTGT...

We employ two Tight-Binding (TB) approaches to study the electronic structure and single carrier transfer in such B-DNA polymers, under the hypothesis that an extra hole or electron travels through HOMOs or LUMOs, respectively. (I) Within TB I (description at the base-pair level), we use the HOMO/LUMO on-site energies of base pairs and the HOMO/LUMO hopping integrals between successive base pairs. The TB parameters for TB I are the same as in Refs.^{17,18,41,42}. (II) Within TB II (description at the single-base level), we use the HOMO/LUMO on-site energies of bases and the HOMO/LUMO hopping integrals between (a) two successive bases on the same strand, (b) complementary bases that constitute a monomer, and (c) diagonally located bases of successive monomers, in the directions $5'-5'$ and $3'-3'$. The TB parameters for TB II are taken from Ref.⁴³. In other words, within TB I, a monomer is considered as a single site, characterized by the index μ , while, within TB II, a base is considered as a single site, characterized by the index β . Below, we use a generic site index j , $j = 1, 2, \dots, MD$, where, $j = \mu$ and $MD = N$, for TB I, while, $j = \beta$ and $MD = 2N$, for TB II. MD denotes “matrix dimension”.

A. Stationary States - Time-independent problem

The HOMO/LUMO Hamiltonian of a given B-DNA segment can be written as

$$\hat{H} = \sum_{j=1}^{MD} E^{s(j)} |j\rangle\langle j| + \sum_{\langle j, j' \rangle} t^{s(j, j')} (|j\rangle\langle j'| + h.c.), \quad (2)$$

where $E^{s(j)}$ is the HOMO/LUMO on-site energy of the j -th site [base pair (bp) for TB I or base (b) for TB II], and $t^{s(j,j')} (= t^{s(j',j)*})$ is the HOMO/LUMO hopping integral between the sites j and j' . $\langle j, j' \rangle$ denotes summation over all relevant neighbors. The neighboring sites which are taken into account for each TB approach are described above. For TB I (*wire* model), the Hamiltonian can be written as

$$\hat{H}_W = \sum_{\mu=1}^N E^{bp(\mu)} |\mu\rangle\langle\mu| + \left(\sum_{\mu=1}^{N-1} t^{bp(\mu, \mu+1)} |\mu\rangle\langle\mu+1| + h.c. \right). \quad (3)$$

For TB II (*extended ladder* model), the Hamiltonian can be written as

$$\begin{aligned} \hat{H}_{EL} = & \sum_{\beta=1}^{MD} E^{b(\beta)} |\beta\rangle\langle\beta| \\ & + \left(\sum_{\beta=1}^{MD-2} t^{b(\beta, \beta+2)} |\beta\rangle\langle\beta+2| + h.c. \right) \\ & + \left(\sum_{\beta=1, \text{odd}}^{MD-1} t^{b(\beta, \beta+1)} |\beta\rangle\langle\beta+1| + h.c. \right) \\ & + \left(\sum_{\beta=1, \text{odd}}^{MD-3} t^{b(\beta, \beta+3)} |\beta\rangle\langle\beta+3| + h.c. \right) \\ & + \left(\sum_{\beta=2, \text{even}}^{MD-2} t^{b(\beta, \beta+1)} |\beta\rangle\langle\beta+1| + h.c. \right), \end{aligned} \quad (4)$$

where the second term represents intra-strand, the third intra-base-pair, the fourth inter-strand 5'-5' and the fifth inter-strand 3'-3' hoppings. In the context of TB, we suppose that $\langle j|j' \rangle = \delta_{jj'}$.

The HOMO/LUMO state of the segment can be expressed as

$$|\text{DNA}\rangle = \sum_{j=1}^{MD} v_j |j\rangle. \quad (5)$$

Substituting Eqs. (2) and (5) to the time-independent Schrödinger equation

$$\hat{H} |\text{DNA}\rangle = E |\text{DNA}\rangle, \quad (6)$$

we arrive to a system of MD coupled equations. Within TB I, the system is of the form

$$Eu_\mu = E^{bp(\mu)} v_\mu + t^{bp(\mu, \mu+1)} v_{\mu+1} + t^{bp(\mu, \mu-1)} v_{\mu-1}, \quad (7)$$

for μ even or odd, while, within TB II, the system is of the form

$$\begin{aligned} Ev_\beta = & t^{b(\beta, \beta-2)} v_{\beta-2} + t^{b(\beta, \beta-1)} v_{\beta-1} + E^{b(\beta)} v_\beta + \\ & t^{b(\beta, \beta+1)} v_{\beta+1} + t^{b(\beta, \beta+2)} v_{\beta+2} + t^{b(\beta, \beta+3)} v_{\beta+3}, \end{aligned} \quad (8a)$$

for β odd, i.e., for the bases of strand 1, and

$$\begin{aligned} Ev_\beta = & t^{b(\beta, \beta-3)} v_{\beta-3} + t^{b(\beta, \beta-2)} v_{\beta-2} + t^{b(\beta, \beta-1)} v_{\beta-1} + \\ & E^{b(\beta)} v_\beta + t^{b(\beta, \beta+1)} v_{\beta+1} + t^{b(\beta, \beta+2)} v_{\beta+2}, \end{aligned} \quad (8b)$$

for β even, i.e., for the bases of strand 2. Eqs. (7) and (8) are equivalent to the eigenvalue-eigenvector problem

$$H\vec{v} = E\vec{v}, \quad (9)$$

where H is the hamiltonian matrix of order MD , composed of the TB parameters E^s and t^s , and \vec{v} is the vector matrix composed of the coefficients v_j . For the segments studied in this work, within TB I, H is either a tridiagonal symmetric Toeplitz matrix of order N for type α' polymers, or a tridiagonal symmetric 2-Toeplitz matrix of order N for type β' and type γ' polymers. Within TB II, H is a heptadiagonal 4-Toeplitz matrix of order $2N$, or, seen another way, a tridiagonal block Toeplitz matrix of order $\frac{N}{2}$, with blocks of order 4. The diagonalization of H leads to the determination of the HOMO/LUMO eigenenergy spectra (*eigenspectra*), $\{E_k\}$, $k = 1, 2, \dots, MD$, for which we suppose that $E_1 < E_2 < \dots < E_{MD}$, as well as to the determination of the occupation probabilities for each eigenstate, $|v_{jk}|^2$, where v_{jk} is the j -th component of the k -th eigenvector. $\{v_{jk}\}$ are normalized, and their linear independence is checked in all cases.

Having determined the eigenspectra, we can compute the Density of States (DOS), generally given by

$$g(E) = \sum_k^{MD} \delta(E - E_k). \quad (10)$$

Changing the view of a B-DNA segment from one (e.g. top) to the other (e.g. bottom) side of the growth axis, reflects the hamiltonian matrix H of the segment on its main antidiagonal. This reflected Hamiltonian, H^{equiv} , describes the *equivalent polymer*. H and H^{equiv} are connected by the similarity transformation $H^{\text{equiv}} = P^{-1}HP$, where $P (= P^{-1})$ is the unit antidiagonal matrix of order MD . Therefore, H and H^{equiv} have identical eigenspectra (hence the equivalent polymers' DOS is identical) and their eigenvectors are connected by $v_{jk} = v_{(MD-j+1)k}^{\text{equiv}}$. For the types of B-DNA polymers studied in this work,

$$\text{equiv}(\text{YX} \dots) = \begin{cases} \text{Y}_{\text{compl}} \text{X}_{\text{compl}} \dots, & \text{for odd } N \\ \text{X}_{\text{compl}} \text{Y}_{\text{compl}} \dots, & \text{for even } N \end{cases} \quad (11)$$

For example, for N odd, $\text{ACAC} \dots \equiv \text{TGTG} \dots$, while, for N even, $\text{ACAC} \dots \equiv \text{GTGT} \dots$.

B. Time-dependent problem

To describe the spatiotemporal evolution of an extra carrier (hole/electron), inserted or created (e.g. by oxidation/reduction) in a B-DNA segment, we consider the

HOMO/LUMO state of the segment as

$$|\text{DNA}(t)\rangle = \sum_{j=1}^{MD} C_j(t) |j\rangle, \quad (12)$$

where $|C_j(t)|^2$ is the probability of finding the carrier at the j -th site at time t . Substituting Eqs. (2) and (12) to the time-dependent Schrödinger equation

$$\hat{H} |\text{DNA}(t)\rangle = i\hbar \frac{\partial}{\partial t} |\text{DNA}(t)\rangle, \quad (13)$$

we arrive at a system of MD coupled differential equations of 1st order. With TB I, the system is of the form

$$i\hbar \frac{dC_\mu}{dt} = E^{bp(\mu)} C_\mu + t^{bp(\mu, \mu+1)} C_{\mu+1} + t^{bp(\mu, \mu-1)} C_{\mu-1}, \quad (14)$$

for μ even or odd. With TB II, the system is of the form

$$i\hbar \frac{dC_\beta}{dt} = t^{b(\beta, \beta-2)} C_{\beta-2} + t^{b(\beta, \beta-1)} C_{\beta-1} + E^{b(\beta)} C_\beta + t^{b(\beta, \beta+1)} C_{\beta+1} + t^{b(\beta, \beta+2)} C_{\beta+2} + t^{b(\beta, \beta+3)} C_{\beta+3}, \quad (15a)$$

for β odd, and

$$i\hbar \frac{dC_\beta}{dt} = t^{b(\beta, \beta-3)} C_{\beta-3} + t^{b(\beta, \beta-2)} C_{\beta-2} + t^{b(\beta, \beta-1)} C_{\beta-1} + E^{b(\beta)} C_\beta + t^{b(\beta, \beta+1)} C_{\beta+1} + t^{b(\beta, \beta+2)} C_{\beta+2}, \quad (15b)$$

for β even. Eqs. (14) and (15) are equivalent to a 1st order matrix differential equation of the form

$$\dot{\vec{C}}(t) = -\frac{i}{\hbar} H \vec{C}(t), \quad (16)$$

where $\vec{C}(t)$ is a vector matrix composed of the coefficients $C_j(t)$, $j = 1, 2, \dots, MD$. Eq. (16) can be solved with the eigenvalue method, i.e., by looking for solutions of the form $\vec{C}(t) = \vec{v} e^{-\frac{i}{\hbar} E t} \Rightarrow \dot{\vec{C}}(t) = -\frac{i}{\hbar} E \vec{v} e^{-\frac{i}{\hbar} E t}$. Hence, Eq. (16) leads to the eigenvalue problem of Eq. (9), that is, $H\vec{v} = E\vec{v}$. Having determined the eigenvalues and eigenvectors of H , the general solution of Eq. (16) is

$$\vec{C}(t) = \sum_{k=1}^{MD} c_k \vec{v}_k e^{-\frac{i}{\hbar} E_k t}, \quad (17)$$

where the coefficients c_k are determined from the initial conditions. In particular, if we define the $MD \times MD$ eigenvector matrix V , with elements v_{jk} , then it can be shown that the vector matrix \vec{c} , composed of the coefficients c_k , $k = 1, 2, \dots, MD$, is given by the expression

$$\vec{c} = V^T \vec{C}(0). \quad (18)$$

Suppose that the extra carrier is placed at the l -th site, that is $C_l(0) = 1$, $C_j(0) = 0, \forall j \neq l$. Then,

$$\vec{c} = \begin{bmatrix} u_{l1} \\ \vdots \\ u_{lk} \\ \vdots \\ u_{lMD} \end{bmatrix}. \quad (19)$$

In other words, the coefficients c_k are given by the row of the eigenvector matrix which corresponds to the site the carrier is initially placed at. In this work, within TB I, we choose $l = 1$, i.e., we initially place the extra carrier at the first monomer (*initial condition*), and, within TB II, we choose either $l = 1$ (*initial condition 1*) or $l = 2$ (*initial condition 2*), i.e., we initially place the extra carrier at each base of the first monomer.

From Eq. (17) it follows that the probability to find the extra carrier at the j -th site of a B-DNA segment is

$$|C_j(t)|^2 = \sum_{k=1}^{MD} c_k^2 v_{jk}^2 + 2 \sum_{k=1}^{MD} \sum_{\substack{k'=1 \\ k' < k}}^{MD} c_k c_{k'} v_{jk} v_{jk'} \cos(2\pi f_{kk'} t), \quad (20)$$

where

$$f_{kk'} = \frac{1}{T_{kk'}} = \frac{E_k - E_{k'}}{h}, \quad \forall k > k', \quad (21)$$

are the frequencies ($f_{kk'}$) or periods ($T_{kk'}$) involved in charge transfer. If M is the number of discrete eigenenergies, then, the number of different $f_{kk'}$ or $T_{kk'}$ involved in CT is $S = \binom{M}{2} = \frac{M!}{2!(M-2)!} = \frac{M(M-1)}{2}$. If there are no degenerate eigenenergies (which holds for all cases studied here, but e.g. does not hold in TB I for *cyclic* type α' polymers¹⁸), then $M = MD$. If eigenenergies are symmetric relative to some central value, then, S decreases (there exist degenerate $f_{kk'}$ or $T_{kk'}$). Specifically, in that case, $S = \frac{M^2}{4}$, for even M and $S = \frac{M^2-1}{4}$ for odd M .

From Eq. (20) it follows that the mean over time probability to find the extra carrier at the j -th site is

$$\langle |C_j(t)|^2 \rangle = \sum_{k=1}^{MD} c_k^2 v_{jk}^2. \quad (22)$$

Furthermore, from Eq. (20) it can be shown that the one-sided Fourier amplitude spectrum that corresponds to the probability $|C_j(t)|^2$ is given by

$$|\mathcal{F}_j(f)| = \sum_{k=1}^{MD} c_k^2 v_{jk}^2 \delta(f) + 2 \sum_{k=1}^{MD} \sum_{\substack{k'=1 \\ k' < k}}^{MD} |c_k c_{k'} v_{jk} v_{jk'}| \delta(f - f_{kk'}). \quad (23)$$

A quantity that can be defined to estimate the transfer rate, i.e., simultaneously, the magnitude of charge transfer and the time scale of the phenomenon, is the *pure*

mean transfer rate

$$k_{j'j} = \frac{\langle |C_j(t)|^2 \rangle}{t_{j'j}}. \quad (24)$$

$t_{j'j}$ is the *mean transfer time*, i.e., having placed the carrier initially at site j' , the time it takes for the probability to find the extra carrier at site j , $|C_j(t)|^2$, to become equal to its mean value, $\langle |C_j(t)|^2 \rangle$, for the first time. For the pure mean transfer rates it holds

$$k_{j'j} = k_{jj'} = k_{(MD-j'+1)(MD-j+1)}^{\text{equiv}} = k_{(MD-j+1)(MD-j'+1)}^{\text{equiv}}. \quad (25)$$

III. RESULTS

A. Eigenspectra and occupation probabilities

Let us start by saying that within TB II (TB I), we take the HOMO or LUMO eigenenergies of bases (base pairs) as the on-site energy of a hole or an electron on a base (base pair). Using the HOMO or LUMO energies of the bases that constitute a base pair, we can estimate the HOMO or LUMO energy of the base pair⁴³. Specifically, supposing that $|\psi_{bp}\rangle = \mathcal{C}_1 |\psi_{b1}\rangle + \mathcal{C}_2 |\psi_{b2}\rangle$, and taking the time-independent Schrödinger equation $\hat{H} |\psi_{bp}\rangle = E |\psi_{bp}\rangle$ we find that the base pair eigenenergies are $E_{1,2} = \frac{E_{b1} + E_{b2}}{2} \pm \sqrt{(\frac{E_{b1} - E_{b2}}{2})^2 + t^2}$, where E_{b1} and E_{b2} are the on-site energies of the bases and

$t = \langle \psi_{b1} | \hat{H} | \psi_{b2} \rangle$ is the intra-base-pair hopping integral i.e. between the two bases that constitute a base pair. However, due to the weak hydrogen bonding between the bases that constitute a base pair, t is very small⁴³, of the order of 10 meV. As a result, practically, $E_{1,2} \approx E_{b1}, E_{b2}$ (with accuracy of 1 meV). Hence, we make the *Observation*: Approximately, the HOMO of the base pair is the highest HOMO of the two bases and the LUMO of the base pair is the lowest LUMO of the two bases. This is expressed in Table I, where we show all energies in eV with accuracy of 0.1 eV. Our numerical results for type

TABLE I: On-site HOMO / LUMO energies of B-DNA bases and base pairs⁴³. All energies are given in eV.

base	Adenine Thymine		Guanine Cytosine	
E_H^b	-8.3	-9.0	-8.0	-8.8
E_L^b	-4.4	-4.9	-4.5	-4.3
E_g	3.9	4.1	3.5	4.5
base pair	A-T		G-C	
E_H^{bp}	-8.3		-8.0	
E_L^{bp}	-4.9		-4.5	
E_g	3.4		3.5	

α' , β' , and γ' polymers (cf. Figs. 1, 2, and 3), indicate that, as, increasing N , a polymer is formed, the energy eigenvalues are distributed around the on-site energies of the base pairs within TB I or the bases within TB II. Hence, the HOMO (LUMO) eigenspectrum of a given polymer within TB I corresponds to the upper (lower) part of its eigenspectrum within TB II.

1. type α' polymers

For TB I, an analytical expression for the eigenvalues of type α' polymers exists¹⁸. All eigenvalues are symmetric around the on-site energy E^{bp} of the monomers and lie in the interval $[E^{bp} - 2|t^{bp}|, E^{bp} + 2|t^{bp}|]$. For odd N , the trivial eigenvalue, $E = E^{bp}$, exists. In the left column of Fig. 1 we present the calculated HOMO/LUMO eigenspectra for an example of type α' polymers, poly(dA)-poly(dT). For TB I, an analytical expression can also be found for the eigenvectors¹⁸. The eigenvectors (hence, the occupation probabilities, too) are *eigenspectrum independent*¹⁸, i.e., they do not depend on the TB parameters E^{bp}, t^{bp} . Furthermore, the occupation probabilities display *palindromicity*¹⁸, i.e., the occupation probability of each eigenstate of the μ -th monomer is equal to that of the $(N - \mu + 1)$ -th monomer ($|u_{\mu k}|^2 = |u_{(N-\mu+1)k}|^2$).

For TB II, up to our knowledge, there are no analytical expressions for eigenvalues and eigenvectors. As an example of type α' polymers, we show, in the right column of Fig. 1, the calculated HOMO/LUMO eigen-

spectra of poly(dA)-poly(dT). The eigenvalues are distributed in two subbands of different width, around the on-site energies of the bases. Furthermore, in accordance with the *Observation*, the upper (lower) subband of the HOMO (LUMO) eigenspectrum corresponds to the band calculated with TB I. For TB II, our numerical results for the eigenvectors indicate that, for β odd (strand 1), $|u_{\beta k}|^2 \approx |u_{(2N-\beta)k}|^2$, while, for β even (strand 2), $|u_{\beta k}|^2 \approx |u_{(2N-\beta+2)k}|^2$, i.e., the occupation probabilities of the eigenstates display approximate *strand-palindromicity*. For HOMO poly(dG)-poly(dC), a case where, according to the parameters used here⁴³, the hopping integrals between diagonally located bases of successive monomers in the 3'-3' and 5'-5' directions are equal, strand palindromicity is strict. This also holds for all type α' polymers, if our extended ladder model is reduced to a simple ladder model by neglecting 3'-3' and 5'-5' inter-strand interactions.

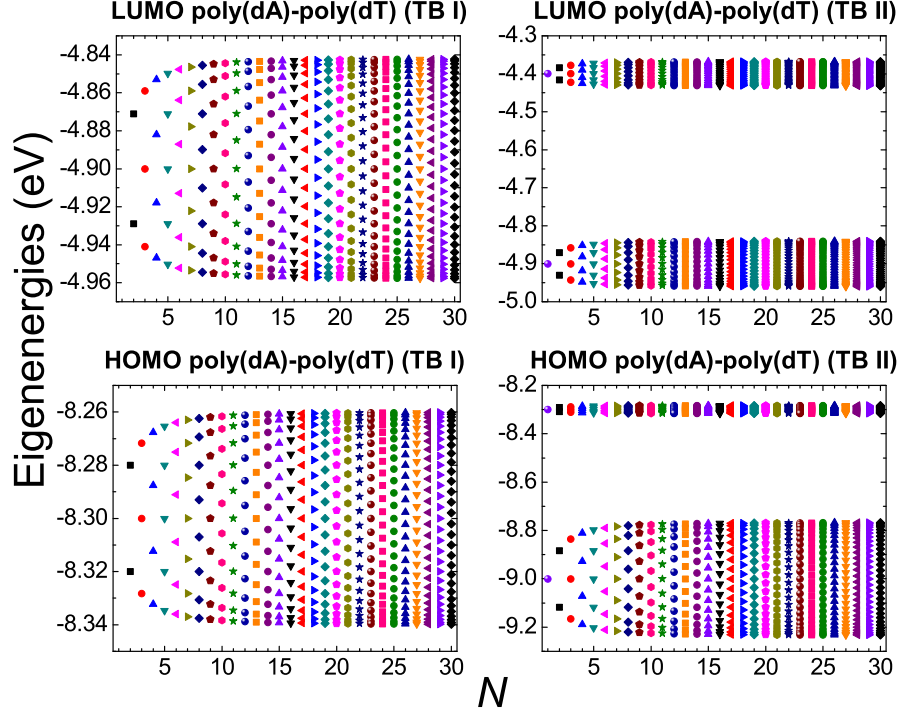


FIG. 1: (Color online) An example of type α' polymers: LUMO (first row) and HOMO (second row) eigenspectra of poly(dA)-poly(dT), for wire model (TB I, first column) and extended ladder model (TB II, second column).

2. type β' polymers

As far as equivalent polymers are concerned, for N even, reflection of the hamiltonian matrix H on its main antidiagonal leads to the same polymers, while for N odd, $\text{GCGC}\dots \equiv \text{CGCG}\dots$, $\text{ATAT}\dots \equiv \text{TATA}\dots$.

For TB I, analytical expressions for the eigenvalues of type β' polymers with N odd exist¹⁸. For N odd the eigenvalues can be expressed explicitly in terms of Chebyshev zeros⁴⁴. All eigenvalues are symmetric around the on-site energy of the monomers, E^{bp} , and the trivial eigenvalue E^{bp} exists. The eigenvalues lie in the interval $[E^{bp} - \sqrt{t_1^2 + t_2^2 + 2|t_1 t_2|}, E^{bp} + \sqrt{t_1^2 + t_2^2 + 2|t_1 t_2|}]$, where t_1, t_2 are the two different hopping integrals e.g., moving from the beginning to the end of the polymer, from-odd-to-even μ and from-even-to-odd μ , respectively. For N even, there is no explicit formula, although a recipe to produce the eigenvalues exists⁴⁴. Our numerical results show that all eigenvalues are symmetric around the on-site energy E^{bp} of the monomers, and lie in the same interval as for N odd. The calculated HOMO/LUMO eigenspectrum for an example of type β' polymers (GCGC...), displaying all the above mentioned properties, is shown in the left column of Fig. 2.

For TB I and N odd, analytical expressions for the eigenvectors exist⁴⁵. These eigenvectors (hence, the occupation probabilities, too) are *partially eigenspectrum dependent*¹⁸, i.e., they depend on t_1, t_2 but not on E^{bp} .

Furthermore, for μ even, the occupation probability of each eigenstate of the μ -th monomer is equal to that of the $(N - \mu + 1)$ -th monomer ($|u_{\mu k}|^2 = |u_{(N-\mu+1)k}|^2$), i.e., for N odd, the occupation probabilities of type β' polymers display *partial palindromicity*¹⁸. Finally, for N odd, equivalence leads to the property $|u_{\mu k}|^2(\text{YX}\dots) = |u_{(N-\mu+1)k}|^2(\text{XY}\dots)$. For N even, we are aware of no analytical expressions for the eigenvectors, but our numerical results show that the occupation probabilities display *palindromicity*¹⁸, i.e., for each eigenstate, the occupation probability of the μ -th monomer is equal to that of the $(N - \mu + 1)$ -th monomer ($|u_{\mu k}|^2 = |u_{(N-\mu+1)k}|^2$).

For TB II, up to our knowledge, there are no analytical expressions for eigenvalues and eigenvectors. As an example of type β' polymers, we show in the right column of Fig. 2 the calculated HOMO/LUMO eigenspectra for GCGC... The eigenvalues are distributed in two subbands of different width, around the on-site energies of the bases. Moreover, in accordance with the *Observation*, the upper (lower) subband of the HOMO (LUMO) eigenspectrum corresponds to the band calculated within TB I. For the TB II eigenvectors, for N odd, equivalence leads to the property $|u_{\beta k}|^2(\text{YX}\dots) = |u_{(2N-\beta+1)k}|^2(\text{XY}\dots)$, while for N even, $|u_{\beta k}|^2 = |u_{(2N-\beta+1)k}|^2$. In other words, the occupation probabilities of the eigenstates display *base-palindromicity*.

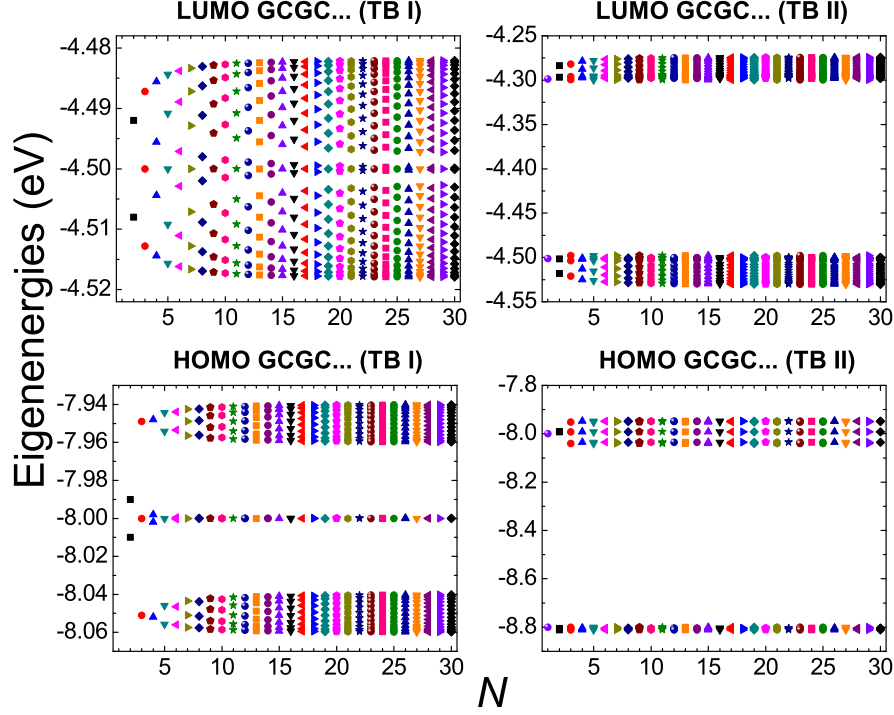


FIG. 2: (Color online) An example of type β' polymers: LUMO (first row) and HOMO (second row) eigenspectra of GCGC..., for wire model (TB I, first column) and extended ladder model (TB II, second column).

3. type γ' polymers

Here, the equivalent polymers are: for N odd, ACAC... \equiv TGTG..., CACA... \equiv GTGT..., CTCT... \equiv GAGA..., TCTC... \equiv AGAG..., and for N even, ACAC... \equiv GTGT..., CACA... \equiv TGTG..., CTCT... \equiv AGAG..., TCTC... \equiv GAGA....

For TB I, analytical expressions for the eigenvalues with N odd exist¹⁸. Let us call $E_{o(e)}^{bp}$ the on-site energy of monomers with μ odd (even), $\Sigma = (E_o^{bp} + E_e^{bp})/2$ and $\Delta = (E_o^{bp} - E_e^{bp})/2$. Then, the eigenvalues include E_o^{bp} , while the rest eigenvalues lie in the interval $[\Sigma - \sqrt{\Delta^2 + t_1^2 + t_2^2 + 2|t_1 t_2|}, \Sigma + \sqrt{\Delta^2 + t_1^2 + t_2^2 + 2|t_1 t_2|}]$. For N even, there is no explicit formula, although a recipe to produce the eigenvalues exists⁴⁴. Our numerical results show that all eigenvalues are symmetric around Σ , and lie in the same interval as for N odd. The calculated HOMO/LUMO eigenspectrum for an example of type γ' polymers (TCTC...), displaying all the above mentioned properties, is shown in the left column of Fig. 3. For TB I and for N odd, analytical expressions can also be found for the eigenvectors⁴⁶. The eigenvectors (hence, the occupation probabilities, too) are *eigenspectrum dependent*¹⁸, i.e., they depend on $E_1^{bp}, E_2^{bp}, t_1, t_2$. Furthermore, for μ even, the occupation probability of each eigenstate of

the μ -th monomer is equal to that of the $(N - \mu + 1)$ -th monomer ($|u_{\mu k}|^2 = |u_{(N-\mu+1)k}|^2$), i.e., for N , odd, the occupation probabilities of type γ' polymers display *partial palindromicity*. For N odd, equivalence leads to $|u_{\mu k}|^2(\text{YX}...) = |u_{(N-\mu+1)k}|^2(\text{Y}_{\text{compl}}\text{X}_{\text{compl}}...)$. For N even, up to our knowledge, no analytical expressions for the eigenvectors exist, but equivalence leads to $|u_{\mu k}|^2(\text{YX}...) = |u_{(N-\mu+1)k}|^2(\text{X}_{\text{compl}}\text{Y}_{\text{compl}}...)$. Our numerical results show that, for all μ , $|u_{\mu k}|^2(\text{YX}...) = |u_{\mu(N-k+1)}|^2(\text{X}_{\text{compl}}\text{Y}_{\text{compl}}...)$.

For TB II, there are no analytical expressions in the literature for eigenvalues and eigenvectors, as far as we know. The calculated HOMO/LUMO eigenspectra for an example of type β' polymers (TCTC...) are demonstrated in the right column of Fig. 3. The eigenvalues are distributed in four subbands of different width, around the on-site energies of the bases. Moreover, in accordance with the *Observation*, the two upper (lower) TB II subbands of the HOMO (LUMO) eigenspectrum correspond to the bands calculated with TB I. For the TB II eigenvectors, equivalence leads to the properties $|u_{\beta k}|^2(\text{YX}...) = |u_{(2N-\beta+1)k}|^2(\text{Y}_{\text{compl}}\text{X}_{\text{compl}}...)$, for N odd, and $|u_{\beta k}|^2(\text{YX}...) = |u_{(2N-\beta+1)k}|^2(\text{X}_{\text{compl}}\text{Y}_{\text{compl}}...)$, for N even. Our numerical results indicate that there are no palindromic properties.

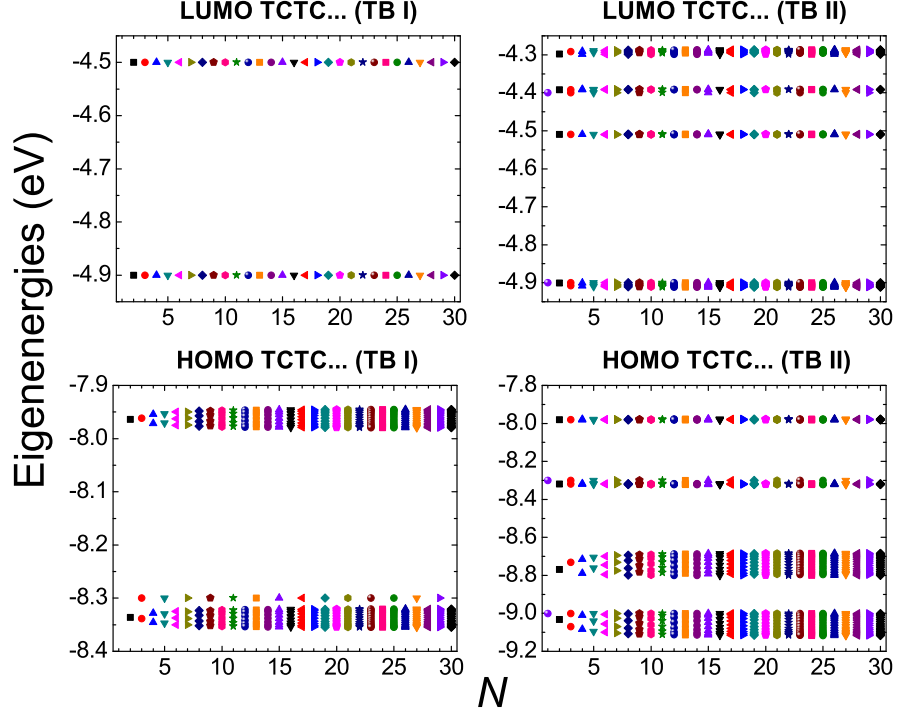


FIG. 3: (Color online) An example of type γ' polymers: LUMO (first row) and HOMO (second row) eigenspectra of TCTC..., for wire model (TB I, first column) and extended ladder model (TB II, second column).

B. Density of States

For TB I or TB II, the DOS can be determined directly by the eigenspectra (cf. Eq. (10)). It represents nicely the corresponding eigenspectral properties (cf. § III A). In Figs. 4, 5, and 6, we illustrate the numerically determined DOS for some representative examples of type α' , β' , and γ' polymers, respectively, for $N = 10^5$, i.e., in the large N limit. We observe that, due to the fact that the eigenenergies become denser and denser as we approach the band or subband edges, van Hove Singularities (vHS) occur at the edges of each band or subband. We also notice that, in the large N limit, the polymer boundaries play insignificant role in the electronic structure, hence, for the same set of TB parameters, the polymers' DOS is essentially the same. For example, in the large N limit, either GCGC... or CGCG..., either N odd or N even have practically the same DOS. In some simpler cases, the DOS can be analytically obtained. For example, for type α' polymers, within TB I, in the large N limit and using periodic boundaries, i.e., for *cyclic* type α' polymers¹⁸,

$$g(E) = \frac{N}{\pi \sqrt{4(tbp)^2 - (E - E^{bp})^2}}. \quad (26)$$

For TB I, the numerically derived DOS for type α' polymers (cf. Fig. 4) is in accordance with Eq. (26), because in the large N limit the boundary conditions play insignificant role. In Fig. 4, for TB I, there is no

minigap, but for TB II there is a minigap of ≈ 0.545 eV; in accordance with the *Observation*, the upper subband of the HOMO band calculated with TB II, corresponds to the HOMO band calculated with TB I. The minigap is mainly due to the different HOMO on-site energies of the two bases (-8.0 eV for G, -8.8 eV for C)⁴³.

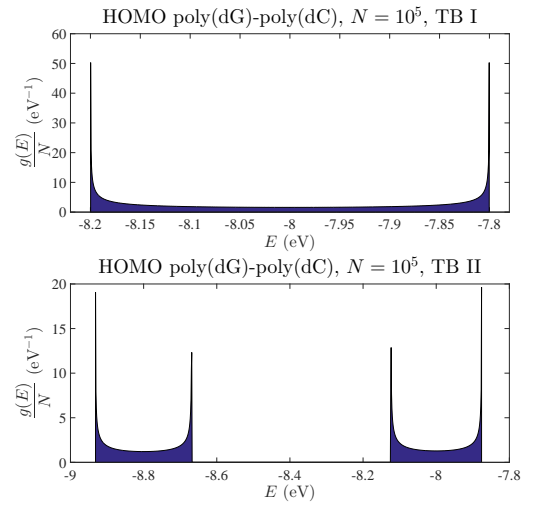


FIG. 4: (Color online) DOS for an example of type α' polymers, poly(dG)-poly(dC) ($N = 10^5$, HOMO), for the base-pair (TB I, top) and the single-base (TB II, bottom) approaches.

A DOS example in type β' polymers is shown in Fig. 5. For TB I, there is a small (≈ 0.004 eV) minigap. For TB II, there is a minigap of ≈ 0.200 eV; in accordance with the *Observation*, the lower subband of the LUMO band calculated with TB II corresponds to the LUMO band calculated with TB I. For TB II, there are two additional small (≈ 0.003 eV, 0.001 eV) minigaps, hardly noticeable at this scale. The underlined TB II minigap corresponds to the TB I minigap, also underlined. For TB II, apart from the vHSs at the subband edges, there is one vHS inside the second subband, hardly seen at this scale.

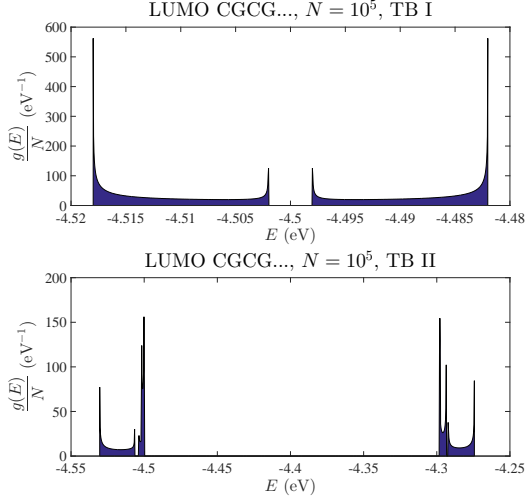


FIG. 5: (Color online) DOS for an example of type β' polymers, CGCG... ($N = 10^5$, LUMO), for the base-pair (TB I, top) and the single-base (TB II, bottom) approaches.

A DOS example in type γ' polymers is shown in Fig. 6. For TB I, there is a minigap a little greater than 0.340 eV, mainly due to the different HOMO on-site energies of the two base pairs (-8.0 eV for G-C, -8.3 eV for A-T)⁴³. For TB II, four minibands are formed approximately around the HOMO on-site energies of the four bases (-9.0 eV for T, -8.8 eV for C, -8.3 eV for A and -8.0 eV for G)⁴³, with three relevant minigaps (0.205 eV, 0.362 eV, 0.334 eV). Two of these minibands are very narrow. In accordance with the *Observation*, the higher two subbands of the HOMO band calculated with TB II correspond to the HOMO band calculated with TB I. The underlined TB II minigap corresponds to the TB I minigap, also underlined.

C. HOMO-LUMO gaps

In Fig. 7, we present the HOMO-LUMO energy gaps, in the large N limit, for all types of polymers. Both TB approaches predict similar gaps, in the range ≈ 3.04 - 3.42 eV. For TB I, the HOMO-LUMO gaps can also be derived analytically, from the maxima and minima of the HOMO and LUMO eigenspectra, respectively (cf. § III A). We also compare the polymer gaps with the two

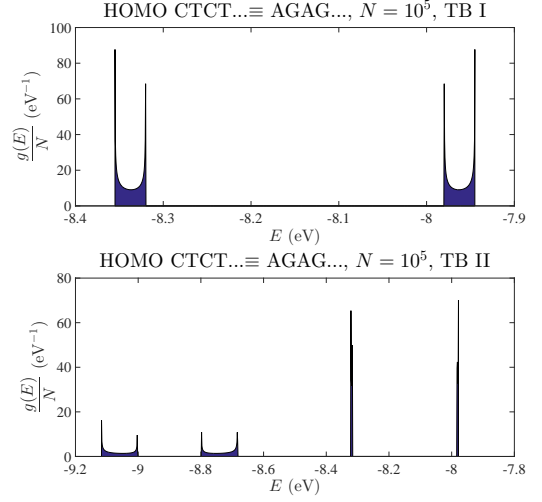


FIG. 6: (Color online) DOS for an example of type γ' polymers, CTCT... \equiv AGAG... ($N = 10^5$, HOMO) for the base-pair (TB I, top) and the single-base (TB II, bottom) approaches.

possible monomer gaps. The decrease of the energy gap, as we move from monomer to polymer, is larger for type γ' polymers.

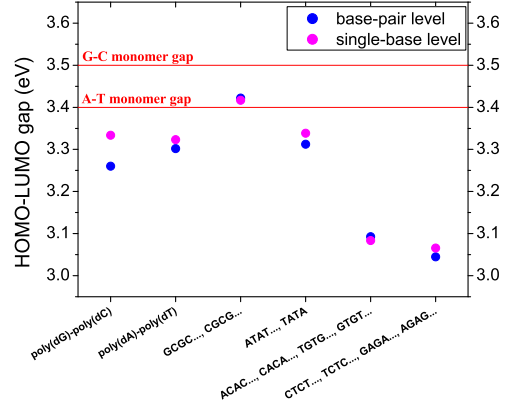


FIG. 7: (Color online) HOMO-LUMO gaps of type α' , β' , and γ' polymers, for the base-pair (TB I, blue dots) and the single-base (TB II, purple dots) approaches. The red lines denote the HOMO-LUMO gaps of the two possible monomers.

D. Mean over time probabilities

Within TB I, from Eq. (20) and the *initial condition* (carrier initially placed at the first monomer), it follows that the mean over time probability to find the extra carrier at the μ -th monomer is

$$\langle |C_\mu(t)|^2 \rangle = \sum_{k=1}^N v_{1k}^2 v_{\mu k}^2. \quad (27)$$

Within TB II, from Eq. (20) and the *initial condition 1* (carrier initially placed at the first base) or the *initial condition 2* (carrier initially placed at the second base), it follows that the mean probability to find the extra carrier at the β -th base is

$$\langle |C_\beta(t)|^2 \rangle = \begin{cases} \sum_{k=1}^{2N} v_{1k}^2 v_{\beta k}^2 \\ \sum_{k=1}^{2N} v_{2k}^2 v_{\beta k}^2 \end{cases}. \quad (28)$$

From Eqs. (27) and (28), we conclude that the *palindromicity* and *eigenspectrum (in)dependence* properties for the occupation probabilities, presented in § III A, hold also for the mean over time probabilities. Finally, for equivalent polymers it can be shown that in TB I $\langle |C_N(t)|^2 \rangle_{\text{YX}\dots} = \langle |C_N(t)|^2 \rangle_{\text{equiv}(\text{YX}\dots)}$, while in TB II $\langle |C_{2N}(t)|^2 \rangle_{\text{YX}\dots} = \langle |C_{2N}(t)|^2 \rangle_{\text{equiv}(\text{YXYX}\dots)}$ (for initial condition 1) and $\langle |C_{2N-1}(t)|^2 \rangle_{\text{YXYX}\dots} = \langle |C_{2N-1}(t)|^2 \rangle_{\text{equiv}(\text{YXYX}\dots)}$ (for initial condition 2).

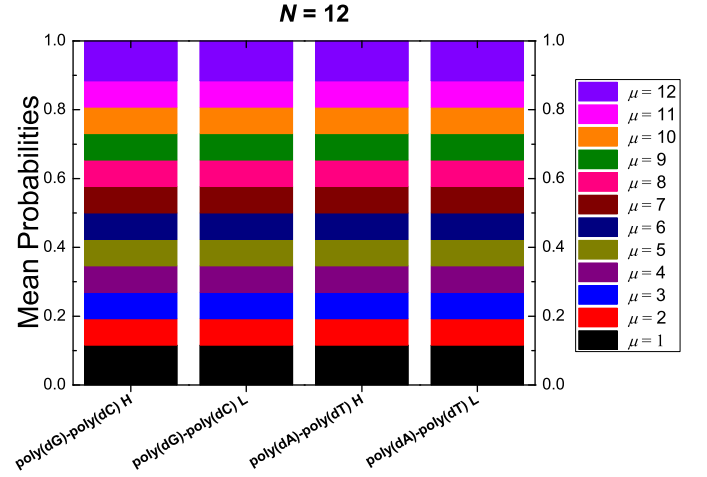


FIG. 8: (Color online) Type α' polymers. TB I and *initial condition* (extra carrier initially at the first base pair). Mean over time probabilities to find an extra hole (HOMO) or electron (LUMO) at each base pair. Here $N = 12$.

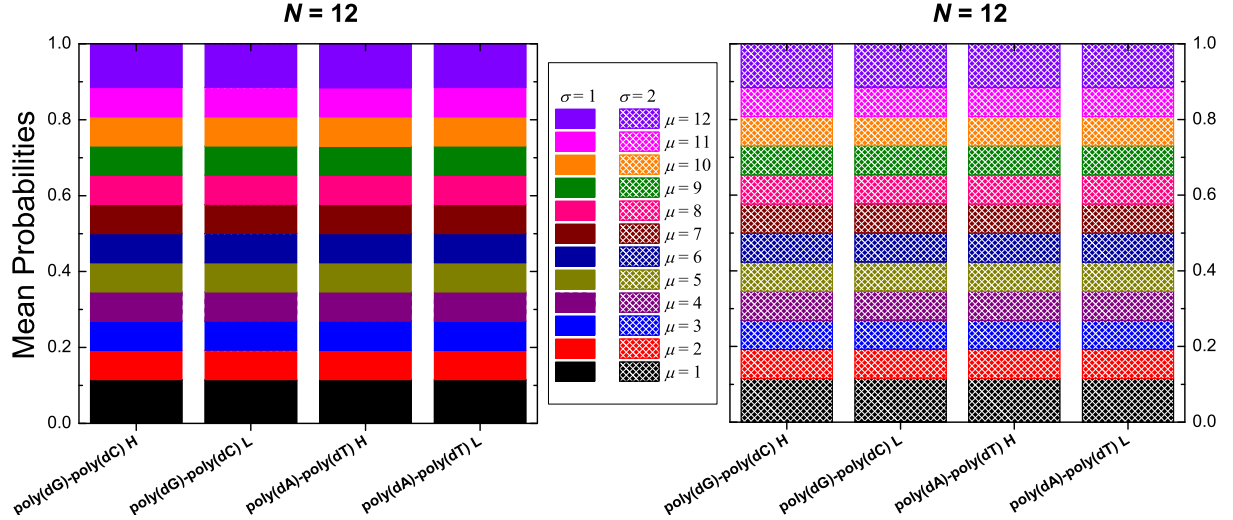


FIG. 9: (Color online) Type α' polymers. TB II and either *initial condition 1* (left) or *initial condition 2* (right), i.e., extra carrier initially at the first or the second base of the first base pair, respectively. Mean over time probabilities to find an extra hole (HOMO) or electron (LUMO) at each base. Here $N = 12$.

1. type α' polymers

In Figs. 8-9, we show an example (for $N = 12$) of our numerical results for the mean over time probabilities to find an extra hole or electron at (I) each base pair according to TB I and the *initial condition* (Fig. 8), and (II) each base according to TB II and the *initial condition 1* or the *initial condition 2* (Fig. 9), for type α' polymers.

For TB I, the mean over time probabilities to find the

carrier at a specific monomer display *palindromicity* and *eigenspectrum independence*¹⁸. Specifically, it can analytically be shown that

$$\langle |C_1(t)|^2 \rangle = \langle |C_N(t)|^2 \rangle = \frac{3}{2(N+1)}, \forall N \geq 2, \quad (29a)$$

$$\langle |C_2(t)|^2 \rangle = \dots = \langle |C_{N-1}(t)|^2 \rangle = \frac{1}{N+1}, \forall N \geq 3. \quad (29b)$$

For TB II, the mean over time probabilities to find the carrier at a specific base display *approximate strand-palindromicity*. Moreover, adding the mean probabilities of the bases that constitute each monomer, it follows that the mean probabilities to find the carrier at a specific monomer are approximately palindromes and almost identically equal, for all cases, to the mean probabilities within TB I, which are strictly palindromes (cf. Eq. (29)). This quantitative agreement suggests that the eigenspectrum independence predicted within the simpler TB I approach, leads to essentially the same results as those derived by the more complicated TB II approach. In Fig. 9 we observe that, within TB II, the carrier moves almost exclusively through the strand it was initially placed at, i.e. carrier movement is mainly of intra-strand character. Furthermore, within TB II, our results for the two initial conditions are in complete agreement.

2. type β' polymers

In Figs. 10-11 we present examples of our numerical results for type β' polymers, for the mean over time probabilities to find an extra hole or electron (I) at each base pair according to TB I and the *initial condition* (Fig. 10), and (II) at each base according to TB II and the *initial condition 1* or the *initial condition 2* (Fig. 11).

For TB I, the mean probabilities to find the carrier at a specific monomer display¹⁸ *partial eigenspectrum dependence* (i.e., dependence on the hopping parameters but not on the on-site energy), *partial palindromicity* (i.e., only for even μ) for N odd and *palindromicity* (i.e., for all μ) for N even.

For TB II, for N even, the mean probabilities to find the carrier at a specific base display *base-palindromicity*. Moreover, adding the mean probabilities of the bases that constitute each base pair, the mean probabilities to find the carrier at a specific base pair are palindromes, in accordance with the prediction of TB I. In Fig. 11, we observe that within TB II, the carrier moves prefer-

ably through the bases that are identical with the one it was initially placed at, in other words it moves crosswise through identical bases, i.e., carrier movement is mainly of inter-strand character.

For N odd, both TB approaches show that there are some cases, in which the carrier hardly moves from its initial site. If we add or subtract a monomer, i.e. for N even, both TB approaches show that a large percentage of the carrier is transferred at the end monomer. Furthermore, both TB approaches show that the mean probability to find the carrier at the last monomer is generally bigger for N even than for N odd.

3. type γ' polymers

In Figs. 12 and 13, we present examples of our numerical results for the mean over time probabilities to find an extra hole or electron (I) at each base pair according to TB I and the *initial condition* (Fig. 12), and (II) at each base according to TB II and the *initial condition 1* or the *initial condition 2* (Fig. 13), for type γ' polymers.

In TB I, given that $|u_{\mu k}|^2(YX\dots) = |u_{\mu(N-k+1)}|^2(X_{\text{compl}}Y_{\text{compl}}\dots)$, for all μ , Eq. (27) leads to identical mean probabilities for (i) TCTC... and GAGA..., (ii) CTCT... and AGAG..., (iii) ACAC... and GTGT..., and (iv) CACA... and TGTG....

In Fig. 12 we observe that within TB I, the carrier moves preferably through the monomers that are identical with the one it was initially placed at, i.e., from the first monomer to the third, and so forth. Within TB II, the carrier moves preferably through the bases that are identical with the one it was initially placed at, i.e., it moves through the same strand from the one or the other base of the first monomer to the identical base of the third monomer, and so forth, i.e., carrier movement is mainly of inter-strand character.

Both TB approaches show that the mean probability to find the carrier at the last monomer is bigger for N odd than for N even, cf. Figs. 12-13.

E. Charge transfer frequency content

For TB I, for type α' and β' polymers, all eigenvalues are symmetric around the on-site energy of the base pairs. Hence, the total number of frequencies involved in charge transfer is $\frac{N^2-1}{4}$ for N odd and $\frac{N^2}{4}$ for N even. For type γ' polymers with N even, the eigenvalues are symmetric around $\frac{E_1^{bp}+E_2^{bp}}{2}$, hence the total number of frequencies is $\frac{N^2}{4}$, too. For type γ' polymers with N odd, the eigenvalues include E_1^{bp} and the total number of frequencies is $\frac{(N-1)(N+3)}{4}$. For TB II, there are no symmetries like those mentioned for TB I, hence the total number of fre-

quencies for all types of polymers (α' , β' , γ') is $N(2N-1)$. From Eq. (23) it follows that all the palindromicity and equivalence properties presented in § III D for the mean over time probabilities, $\langle |C_j(t)|^2 \rangle$, hold for the Fourier spectra, $|\mathcal{F}_j(f)|$, too. In the following Subsections, we focus on the Fourier spectra that correspond to charge transfer from the first to the last monomer i.e. on $|\mathcal{F}_1(f)|$ and $|\mathcal{F}_N(f)|$ for TB I, and on $|\mathcal{F}_1(f)|$, $|\mathcal{F}_2(f)|$, $|\mathcal{F}_{2N-1}(f)|$ and $|\mathcal{F}_{2N}(f)|$ for TB II. Both TB approaches show that the frequency content is mainly in the THz domain, cf. Figs. 14, 15, 16, 17, 18, 19.

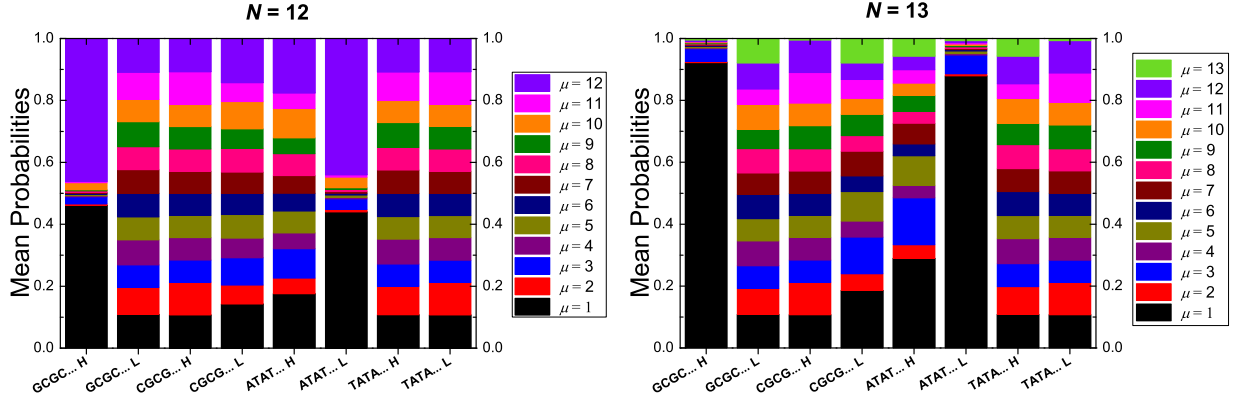


FIG. 10: (Color online) Type β' polymers. TB I and *initial condition* (extra carrier initially at the first base pair). Mean over time probabilities to find an extra hole (HOMO) or electron (LUMO) at each base pair. N even (here $N = 12$, left) or N odd (here, $N = 13$, right).

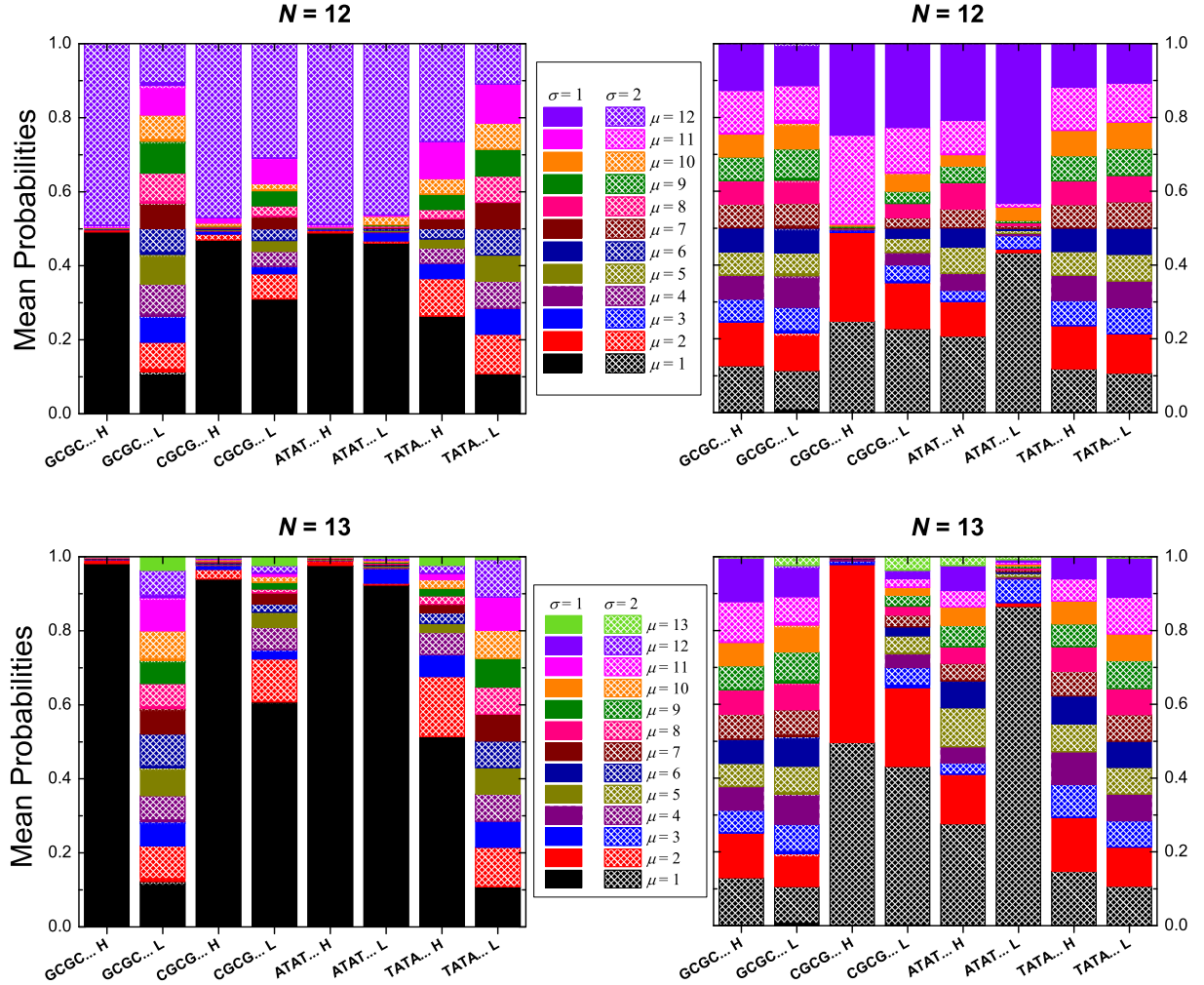


FIG. 11: (Color online) Type β' polymers. TB II and either *initial condition 1* (left) or *initial condition 2* (right), i.e., extra carrier initially at the first or the second base of the first base pair, respectively. Mean over time probabilities to find an extra hole (HOMO) or electron (LUMO) at each base. N even (upper panels, here $N = 12$) or N odd (lower panels, here $N = 13$).

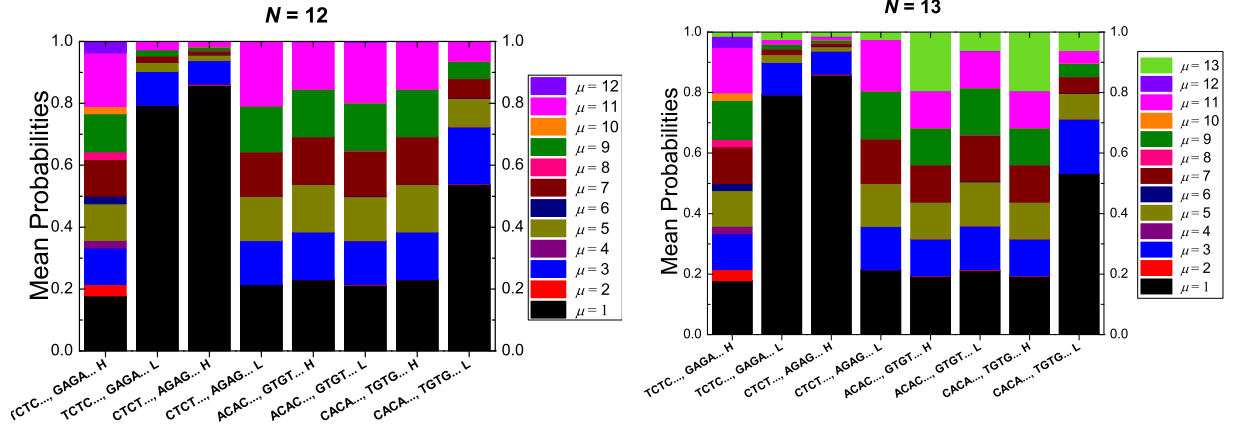


FIG. 12: (Color online) Type γ' polymers. TB I and *initial condition* (extra carrier initially at the first base pair). Mean over time probabilities to find an extra hole (HOMO) or electron (LUMO) at each base pair. N even (here $N = 12$, left) or N odd (here $N = 13$, right).

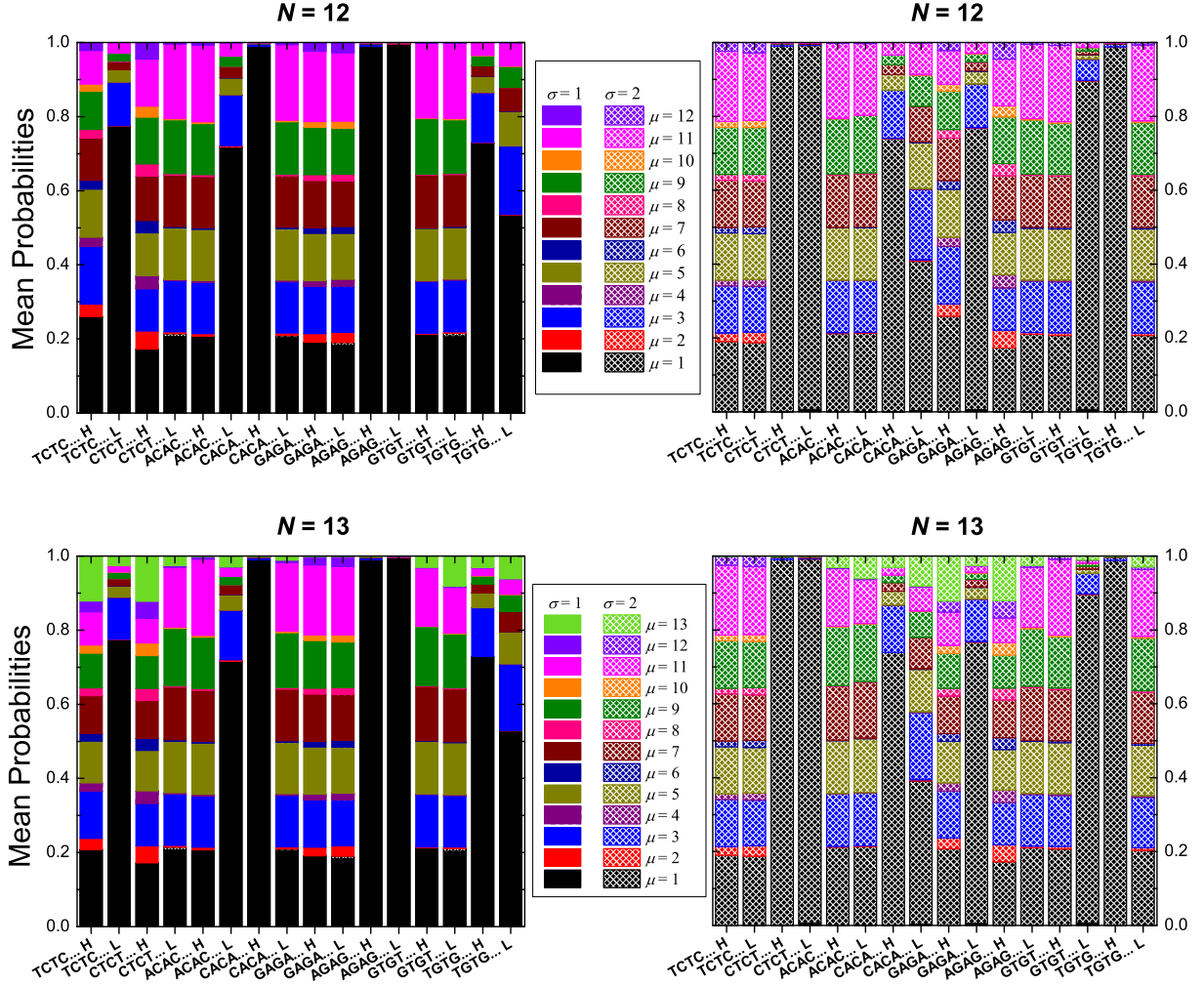


FIG. 13: (Color online) Type γ' polymers. TB II and either *initial condition 1* (left) or *initial condition 2* (right), i.e., extra carrier initially at the first or the second base of the first base pair, respectively. Mean over time probabilities to find an extra hole (HOMO) or electron (LUMO) at each base. N even (upper panels, here $N = 12$) or N odd (lower panels, here $N = 13$).

1. type α' polymers

Within TB I the main frequencies are in the range $\approx 0.3 - 97$ THz. Within TB II, they are in the range $\approx 0.1 - 110$ THz. The main frequency content is between far-infrared (FIR) and mid-infrared (MIR). As an example, we show in Fig. 14 (TB I and *initial condition*) and Fig. 17 (TB II and *initial condition 1* or *initial condition 2*), the Fourier spectra, at the first and the last monomer, of an extra hole in poly(dA)-poly(dT) with $N = 20$. In Fig. 14 we observe that the Fourier amplitudes for the first and the last monomer are approximately equal, mirroring the efficient hole transfer in poly(dA)-poly(dT), cf. also Fig. 8. Inspection of Fig. 17 leads to the same conclusion. Additionally, Fig. 17 underlines the intra-strand character of carrier transfer and shows that initial conditions 1 and 2 lead to similar form of Fourier spectra.

2. type β' polymers

Within TB I, the main frequencies are in the range $\approx 0.01 - 40$ THz, i.e., between microwaves (MW) and MIR. Within TB II, they are in the range $\approx 0.01 - 210$ THz, i.e., between the MW and near-infrared NIR. As an example, we show in Fig. 15 (TB I and *initial condition*) and Fig. 18 (TB II and *initial condition 1* or *initial condition 2*), the Fourier spectra, at the first and the last monomer, of an extra electron in ATAT... with $N = 14$. In Fig. 15 we observe that the Fourier amplitudes for the first and the last monomer are approximately equal, mirroring the finally large electron transfer in ATAT... for N even, cf. also Fig. 10. However, this large transfer is very slow, its main frequency is very small but with a large amplitude. The same conclusions can be drawn from Fig. 18, where we can additionally observe the inter-strand character of charge transfer and that initial conditions 1 and 2 lead to similar form of Fourier spectra.

3. type γ' polymers

Within TB I, the main frequencies are in the range ≈ 0.4 GHz - 40 THz, i.e., between radiowaves (RW) and MIR. Within TB II, they are in the range $\approx 0.02 - 190$ THz, i.e., between MW and FIR. As an example, we show in Fig. 16 (TB I and *initial condition*) and Fig. 19 (TB II and *initial condition 1* or *initial condition 2*), the Fourier spectra, at the first and the last monomer, of an extra hole in TCTC... with $N = 21$. In Fig. 16 we observe that the Fourier amplitudes for the first monomer are much larger than the ones for the last monomer, mirroring the inefficient hole transfer in TCTC... for N odd, cf. also Fig. 12. In Fig. 19, we can additionally observe the intra-strand character of charge transfer and that initial conditions 1 and 2 lead to somehow different form of Fourier spectra, initial condition 1 being more

efficient than initial condition 2 for hole transfer, cf. also Figs. 12 and 13.

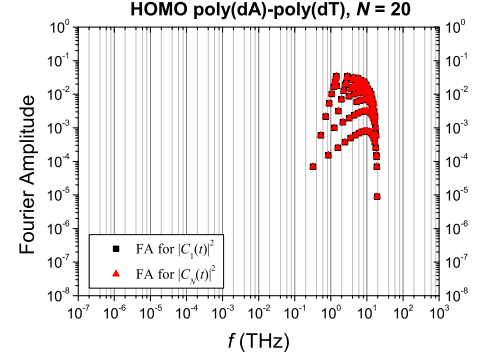


FIG. 14: (Color online) Type α' polymers, here poly(dA)-poly(dT), $N = 20$. TB I and *initial condition* (extra carrier initially at the first base pair). Hole transfer Fourier spectra at the first and the last monomer.

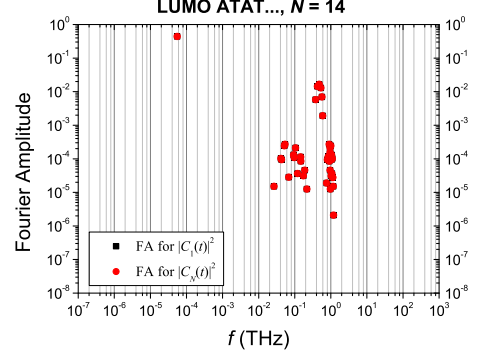


FIG. 15: (Color online) Type β' polymers, here ATAT..., $N = 14$. TB I and *initial condition* (extra carrier initially at the first base pair). Electron transfer Fourier spectra at the first and the last monomer.

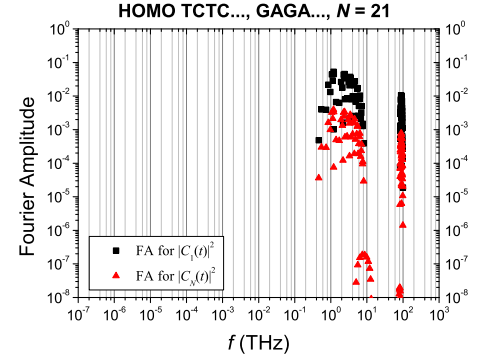


FIG. 16: (Color online) Type γ' polymers, here TCTC..., $N = 21$. TB I and *initial condition* (extra carrier initially at the first base pair). Hole transfer Fourier spectra at the first and the last monomer.

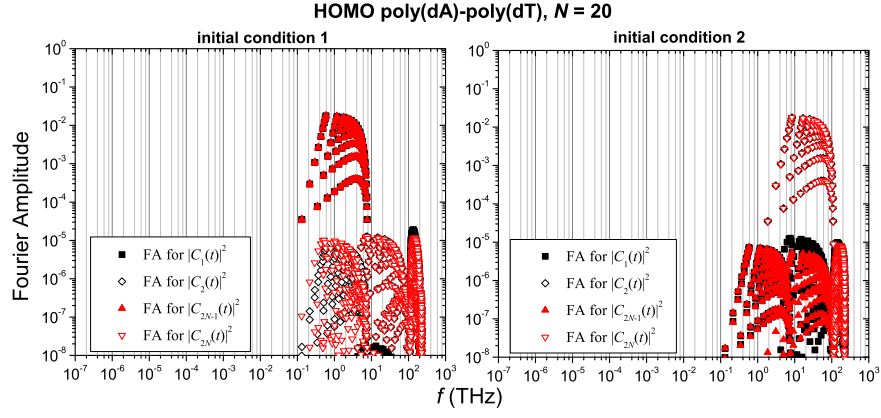


FIG. 17: (Color online) Type α' polymers, here poly(dA)-poly(dT), $N = 20$. TB II and either *initial condition 1* (left) or *initial condition 2* (right). Hole transfer Fourier spectra at the first and the last monomer.

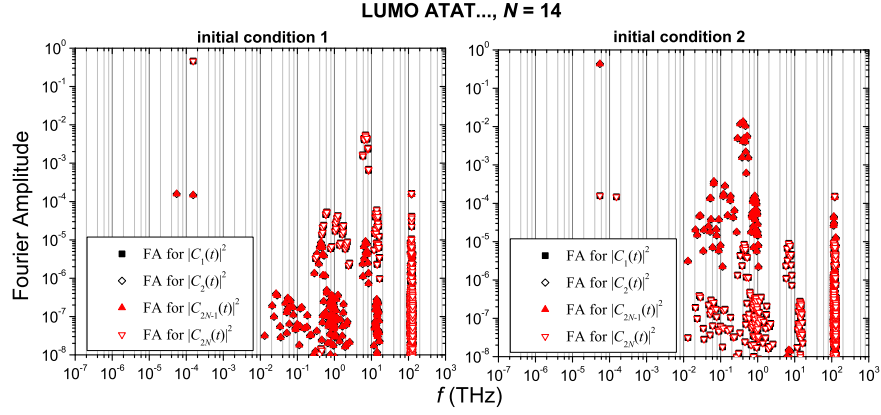


FIG. 18: (Color online) Type β' polymers, here ATAT..., $N = 14$. TB II and either *initial condition 1* (left) or *initial condition 2* (right). Electron transfer Fourier spectra at the first and the last monomer.

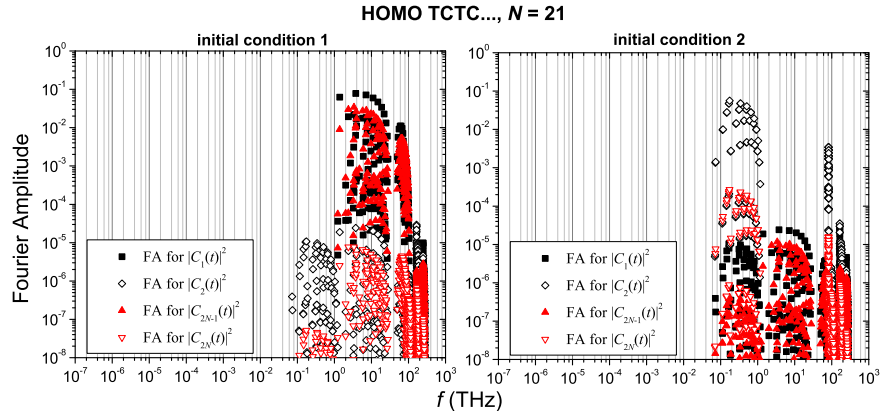


FIG. 19: (Color online) Type γ' polymers, here TCTC..., $N = 21$. TB II and either *initial condition 1* (left) or *initial condition 2* (right). Hole transfer Fourier spectra at the first and the last monomer.

F. Pure mean transfer rates

In the following subsections we focus on pure mean transfer rates between the first and the last monomer,

either within TB I or within TB II.

1. type α' polymers

As a characteristic example, we present in Fig. 20 the hole pure mean transfer rates for poly(dG)-poly(dC), from the first to the last monomer, either within TB I or within TB II. Specifically, (I) for TB I we illustrate $k_{1,N}$ on the left panel, and (II) for TB II we illustrate $k_{1,2} = k_{2,1}$, $k_{1,2N-1} = k_{2,2N}$ and $k_{1,2N} = k_{2,2N-1}$ on the right panel. We have already noticed in § III D 1 that, within TB II, carrier transfer is almost exclusively of intra-strand character. Hence, within TB II, $k_{1,2N-1} = k_{2,2N}$ are the largest transfer rates. Comparing $k_{1,N}$ for TB I with $k_{1,2N-1} = k_{2,2N}$ for TB II, we observe an excellent agreement, both qualitatively and quantitatively. Within TB II, the intra-base-pair rates $k_{1,2} = k_{2,1}$ are small and the inter-strand rates $k_{1,2N} = k_{2,2N-1}$ insignificant. Increasing N , the intra-strand transfer rates $k_{1,2N-1} = k_{2,2N}$ decrease reaching gradually the level of the intra-base-pair rates $k_{1,2} = k_{2,1}$, at which point, finally, charge transfer along the polymer is insignificant. Increasing N , the insignificant inter-strand rates $k_{1,2N} = k_{2,2N-1}$ also gradually decrease further.

2. type β' polymers

We have already mentioned (cf. § III D 2 and III E 2) that both TB approaches predict that for some cases of type β' polymers, for N even, the carrier is transferred at a large percentage to the last monomer but the transfer is very slow. Such a case is presented in Fig. 21. Specifically, we show the electron pure mean transfer rates for ATAT... from the first to the last monomer, either within TB I or within TB II. Specifically, (I) for TB I, we illustrate $k_{1,N}$ (left), and (II) for TB II, we illustrate the largest transfer rates (right). We have already demonstrated in § III D 2 that, within TB II, the extra carrier is transferred almost exclusively crosswise, through identical bases. Hence, for TB II, the largest transfer rates are $k_{1,2N-1}$ and $k_{2,2N}$ for N odd, and $k_{1,2N}$ and $k_{2,2N-1}$ for N even. We depict these largest transfer rates in Fig. 21 (right). In other cases of type β' polymers the pure mean transfer rates fall over N in a different manner, somehow similar to the behavior of type γ' polymers, which is shown in § III F 3.

3. type γ' polymers

As a characteristic example, we present in Fig. 22 the hole pure mean transfer rates for TCTC..., from the first to the last monomer, either within TB I or within TB II. Specifically, (I) for TB I we illustrate $k_{1,N}$ on the left panel, and (II) for TB II we illustrate $k_{1,2N-1}$ and $k_{2,2N}$ on the right panel. We have already mentioned in § III D 3 that, within TB II, the extra carrier is transferred almost exclusively through the strand it was initially placed at, i.e., for type γ' polymers the charge transfer is mainly of intra-strand character. Hence, for TB II, we show $k_{1,2N-1}$ and $k_{2,2N}$ which are the largest transfer rates. We have demonstrated § III F 1 that, for type α' polymers, $k_{1,2N-1} = k_{2,2N}$. As shown in Fig. 22, this does not hold for type γ' polymers.

4. Pure mean transfer rate fits

Finally, we compare the results of our two TB approaches by performing the exponential fits $k = k_0 e^{-\beta d}$ and $k = A + k_0 e^{-\beta d}$, where $d = (N - 1) \times 3.4 \text{ \AA}$ is the charge transfer distance, as well as the power-law fit, $k = k'_0 N^{-\eta}$. Our results for TB I have already been presented in Figs. 8-9 of Ref.¹⁸. For TB II, we again focus on the pure mean transfer rates between the bases of the initial and the final monomer for which carrier transfer is significant. The conclusions are similar to those within TB I. The fits are considerably improved if polymers with N odd and N even are fitted separately. Moreover, the power-law fits are generally better, in terms of correlation coefficients. Our results for the exponent η of the power-law fits, within TB II, are presented in Fig. 23. Our results confirm the statement that the fall of k as a function of N becomes generally steeper as the intricacy of the energy structure increases, i.e., from type α' to type β' and further to type γ' polymers¹⁸. This conclusion also holds for the exponential fits, which are not presented here. Furthermore, both TB I and TB II show that there is perfect agreement between our results for β and η for all type α' polymers. This leads to the conclusion that although the interaction strength (as reflected in the hopping integrals) is different in each case of type α' polymers leading to different values of k , the way k falls over N or d is the same.

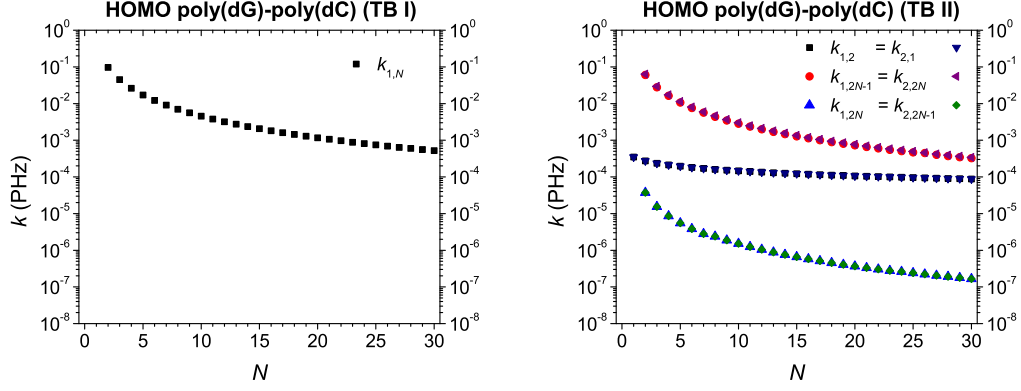


FIG. 20: (Color online) Type α' polymers, here poly(dG)-poly(dC). Hole pure mean transfer rates (I) $k_{1,N}$ for TB I (left), and (II) $k_{1,2} = k_{2,1}$, $k_{1,2N-1} = k_{2,2N}$ and $k_{1,2N} = k_{2,2N-1}$ for TB II (right).

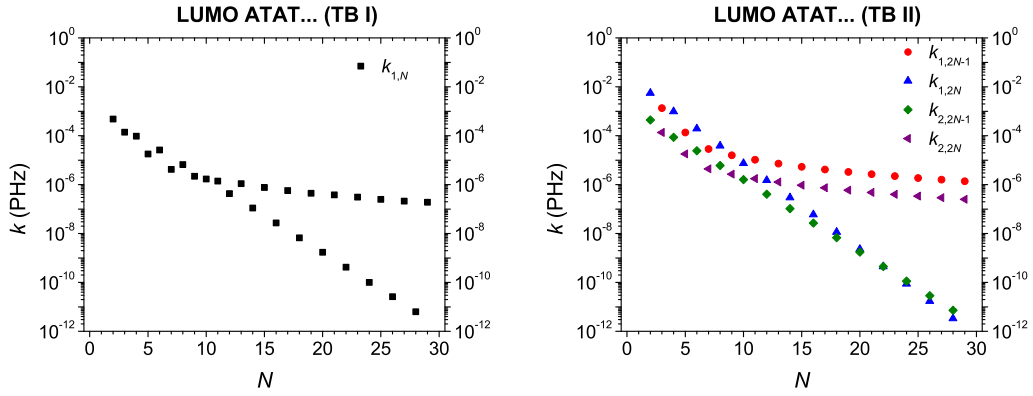


FIG. 21: (Color online) Type β' polymers, here is a case where, for N even, the carrier is transferred at a large percentage to the last monomer but the transfer is very slow: Electron pure mean transfer rates in ATAT..., either $k_{1,N}$ within TB I (left) or the largest transfer rates in TB II, i.e., $k_{1,2N-1}$ for N odd, $k_{1,2N}$ for N even, $k_{2,2N}$ for N odd, $k_{2,2N-1}$ for N even.

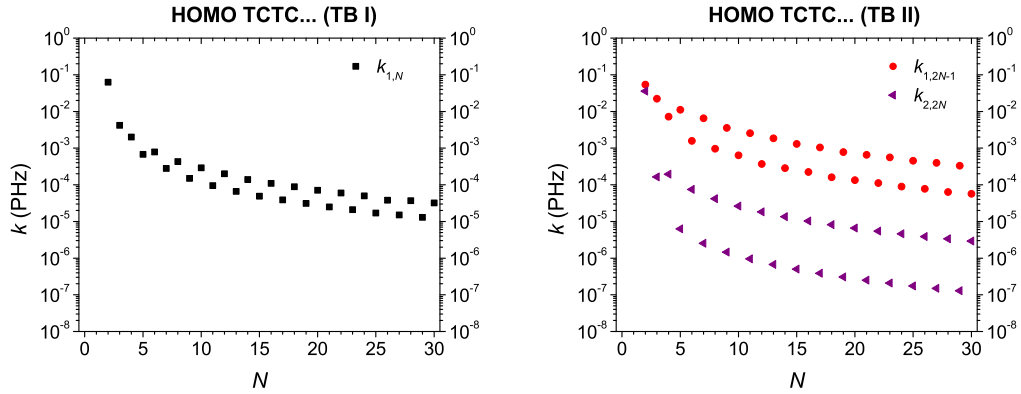


FIG. 22: (Color online) Type γ' polymers, here TCTC... Hole pure transfer rates $k_{1,N}$ for TB I (left), and $k_{1,2N-1}$, $k_{2,2N}$ for TB II (right).

IV. CONCLUSION

We employed two Tight-Binding approaches to examine time-independent and time-dependent aspects of the electronic structure and carrier transfer in B-DNA monomer polymers (type α') and dimer polymers (type β' and type γ'). We used a simplistic wire model (TB I) where a carrier is initially located at a base pair (called also a monomer in this article) and then moves to the next or to the previous base pair, as well as a more detailed extended ladder model (TB II) where the carrier is initially located at a base and then moves to all possible neighboring bases including diagonally located ones. The inclusion of diagonal hoppings is crucial for type β' polymers where carrier transfer is mainly of inter-strand character. The time-dependent and the time-independent problems involve diagonalization of matrices with matrix dimension $MD = N$ for TB I and $MD = 2N$ for TB II. The two TB approaches give coherent, complementary aspects of electronic properties and charge transfer in B-DNA monomer polymers and dimer polymers.

For the time-independent problem, we studied the HOMO and the LUMO eigenspectra and the occupation probabilities, the Density of States and the HOMO-LUMO gap. The upper (lower) subband of the HOMO (LUMO) eigenspectrum calculated with TB II corresponds to the band calculated with TB I. The occupation probabilities within TB I and TB II show various degrees of palindromicity and eigenspectrum (in)dependence of the probabilities to find the carrier at a site. The DOS displays nice van Hove singularities at the (sub)band edges, while the numerically calculated DOS for simple cases agrees with the analytical solution. As expected,

the polymer HOMO-LUMO gaps are smaller than the HOMO-LUMO gaps of the two possible monomers, reaching a level of 3.4 to 3.0 eV. The smallest HOMO-LUMO gaps occur for type γ' polymers.

For the time-dependent problem we investigated the mean over time probabilities to find the carrier at each site (base pair for TB I and base for TB II), the Fourier spectra and the pure mean transfer rates from a certain site to another. The mean over time probabilities illustrate clearly the basically intra-strand character of carrier transfer in type α' and type γ' polymers. However, while in type α' polymers the carrier moves successively through all bases of the same strand, in type γ' polymers the carrier moves through the bases that are identical with the one it was initially placed at, i.e., it moves through the same strand from the one or the other base of the first monomer to the identical base of the third monomer, and so forth. Carrier transfer is basically of inter-strand character in type β' polymers. The Fourier spectra give us a nice representation of the frequency content of charge transfer. Both TB approaches show that this frequency content is mainly in the THz domain, the details depend on the type of polymers and the TB approach used. The pure mean transfer rates k show both how fast carrier transfer is and how much of the carrier is transferred from the initial site to the final site. The $k(N)$ fits are considerably improved if polymers with N odd and N even are fitted separately. Additionally, the power-law fits are generally better, in terms of correlation coefficients. Our results confirm the statement that the fall of k as a function of N becomes generally steeper as the intricacy of the energy structure increases, i.e., from type α' to type β' and further to type γ' polymers.

* Current affiliation: University of Copenhagen, Niels Bohr Institute, Blegdamsvej 17, DK-2100 Copenhagen, Denmark.

† Current affiliation: Georg-August-Universität Göttingen, Fakultät für Physik, Friedrich-Hund-Platz 1 D-37077 Göttingen, Germany.

‡ Electronic address: csimseri@phys.uoa.gr; URL: http://users.uoa.gr/~csimseri/physics_of_nanostructures_and_biomaterials_in_the

¹ C.C. Page, C.C Moser and P. Leslie Dutton, Mechanism for electron transfer within and between proteins, *Current Opinion in Chemical Biology* **7**, 551 (2003).

² H.B. Gray and J.R. Winkler, Electron flow through metalloproteins, *Biochimica et Biophysica Acta* **1797**, 1563 (2010).

³ C.C. Moser, J.L. Ross Anderson, P. Leslie Dutton, Guidelines for tunneling in enzymes, *Biochimica et Biophysica Acta* **1797**, 1573 (2010).

⁴ J. M. Artés, M. López-Martínez, I. Díez-Pérez, F. Sanz and P. Gorostiza, Nanoscale charge transfer in redox proteins

and DNA: Towards biomolecular electronics, *Electrochimica Acta* **140**, 83 (2014).

⁵ A.M. Kannan, V. Renugopalakrishnan, S. Filipek, P. Li, G.F. Audette, and L. Munukutla, Bio-Batteries and Bio-Fuel Cells: Leveraging on Electronic Charge Transfer Proteins, *J. Nanosci. Nanotechnol.* **9**, 1665 (2009).

⁶ P.J. Dandliker, R. Erik Holmlin, J.K. Barton, Oxidative lesions and DNA repair in the DNA Helix, *Science* **275**, 1465 (1997).

⁷ S.R. Rajski, B.A. Jackson, J.K. Barton, DNA repair: models for damage and mismatch recognition, *Mutation Research* **447**, 49 (2000).

⁸ B. Giese, Electron transfer through DNA and peptides, *Bioorganic & Medicinal Chemistry* **14**, 6139 (2006).

⁹ C.-T. Shih, Y.-Y. Cheng, S.A. Wells, C.-L. Hsu, R.A. Römer, Charge transport in cancer-related genes and early carcinogenesis, *Computer Physics Communications* **182**, 36 (2011).

¹⁰ H.-W. Fink and C. Schönenberger, Electrical conduction

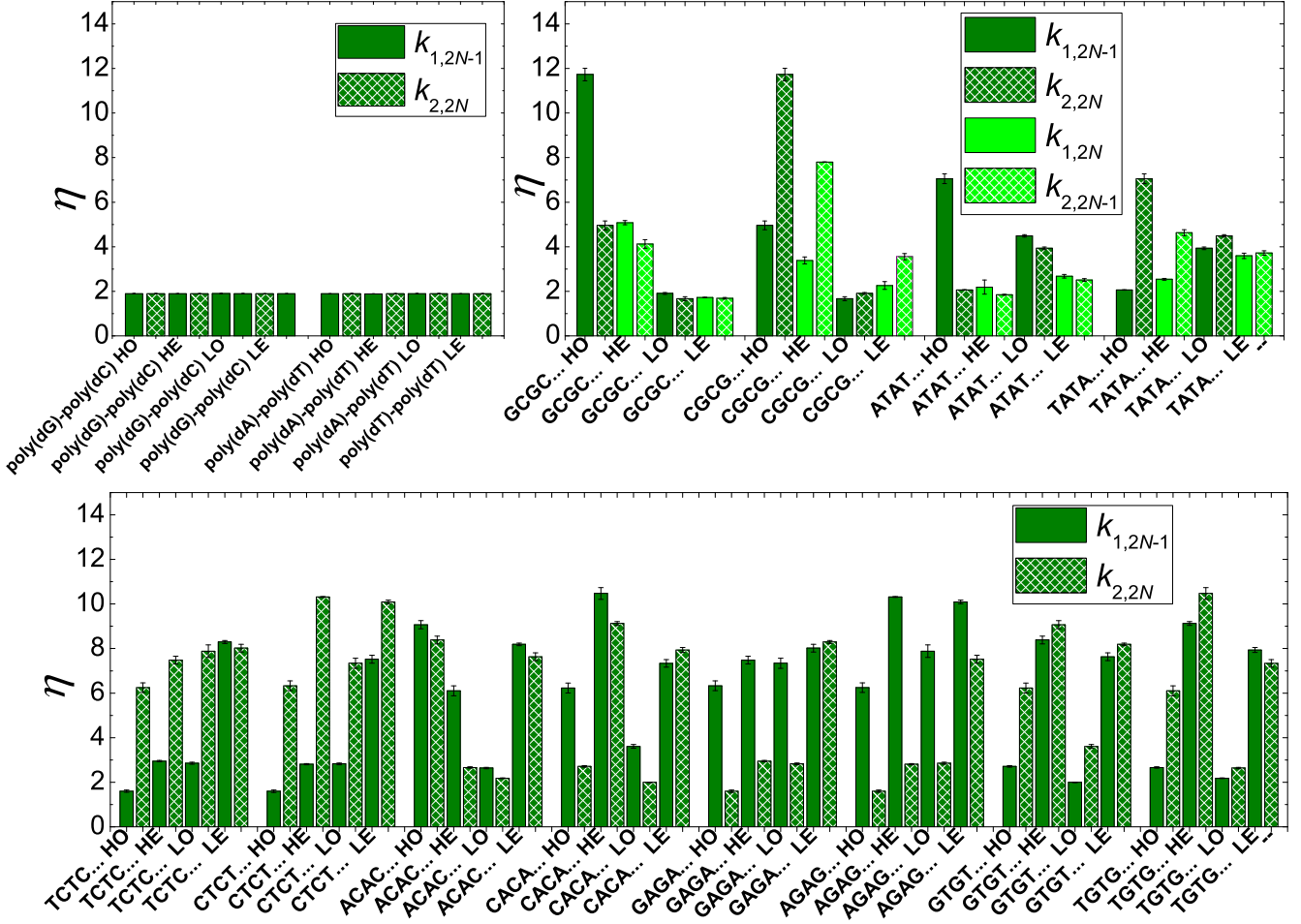


FIG. 23: (Color online) The exponent η of the power-law fits, $k = k'_0 N^{-\eta}$, within TB II.

- through DNA molecules, *Nature* **398**, 407 (1999).
- ¹¹ D. Porath, A. Bezryadin, S. De Vries, and C. Dekker, Direct measurement of electrical transport through DNA molecules, *Nature* **403**, 635 (2000).
 - ¹² A.J. Storm, J. van Noort, S. de Vries, and C. Dekker, Insulating behavior for DNA molecules between nanoelectrodes at the 100 nm length scale, *Appl. Phys. Lett.* **79**, 3881 (2001).
 - ¹³ K.-H. Yoo, D.H. Ha, J.-O. Lee, J.W. Park, J. Kim, J.J. Kim, H.-Y. Lee, T. Kawai, and H.Y. Choi, Electrical Conduction through Poly(dA)-Poly(dT) and Poly(dG)-Poly(dC) DNA Molecules, *Phys. Rev. Lett.* **87**, 198102 (2001).
 - ¹⁴ B. Xu, P. Zhang, X. Li, and N. Tao, Direct Conductance Measurement of Single DNA Molecules in Aqueous Solution, *Nano Lett.* **4**, 1105 (2004).
 - ¹⁵ H. Cohen, C. Nogues, R. Naaman, and D. Porath, Direct measurement of electrical transport through single DNA molecules of complex sequence, *Proc. Nat. Acad. Sci.* **102**, 11589 (2005).
 - ¹⁶ G.P. Triberis, C. Simserides and V.C. Karavolas, Small polaron hopping transport along DNA molecules, *J. Phys.: Condens. Matter* **17** (2005) 2681.
 - ¹⁷ C. Simserides, A systematic study of electron or hole transfer along DNA dimers, trimers and polymers, *Chem. Phys.* **440**, 31 (2014).
 - ¹⁸ K. Lambropoulos, M. Chatzieftheriou, A. Morphis, K. Kaklamanis, M. Theodorakou, and C. Simserides, Unbiased charge oscillations in B-DNA: Monomer polymers and dimer polymers, *Phys. Rev. E* **92**, 032725 (2015).
 - ¹⁹ C.H. Wohlgamuth, M.A. McWilliams, and J.D. Slinker, DNA as a Molecular Wire: Distance and Sequence Dependence, *Anal.Chem.* **85**, 8634 (2013).
 - ²⁰ F.D. Lewis, M.R. Wasielewski, Dynamics and efficiency of photoinduced charge transport in DNA: Toward the elusive molecular wire, *Pure and Applied Chemistry* **85**, 1379 (2013).
 - ²¹ R. Gutierrez, R. Caetano, P.B. Woiczikowski, T. Kubar, M. Elstner and G. Cuniberti, Structural fluctuations and quantum transport through DNA molecular wires: a combined molecular dynamics and model Hamiltonian approach, *New Journal of Physics* **12**, 023022 (2010).
 - ²² K. Kawai, T. Majima, Chapter 44, Increasing the Hole Transfer Rate Through DNA by Chemical Modification, in *Chemical Science of -Electron Systems*, edited by T. Akasaka, A.O.S. Fukuzumi, H.K.Y. Aso, Springer Springer Tokyo Heidelberg New York Dordrecht London (2015).
 - ²³ Y.-J. Ye, L.-L. Shen, DFT Approach to Calculate Elec-

- tronic Transfer through a Segment of DNA Double Helix, *J. Comp. Chem.* **21** (2000) 1109.
- ²⁴ Y.-J. Ye, Y. Jiang, Electronic Structures and Long-Range Electron Transfer Through DNA Molecules, *Int. J. Quant. Chem.* **78** (2000) 112.
 - ²⁵ R.N. Barnett, C.L. Cleveland, U. Landman, E. Boone, S. Kanvah, G.B. Schuster, Effect of Base Sequence and Hydration on the Electronic and Hole Transport Properties of Duplex DNA: Theory and Experiment, *J. Phys. Chem. A* **107** (2003) 3525.
 - ²⁶ E. Artacho, M. Machado, D. Sánchez-Portal, P. Ordejón, and J.M. Soler, Electrons in dry DNA from density functional calculations, *Mol. Phys.* **101** (2003) 1587.
 - ²⁷ C. Adessi, S. Walch, and M.P. Anantram, Environment and structure influence on DNA conduction, *Phys. Rev. B* **67** (2003) 081405(R).
 - ²⁸ H. Mehrez and M. P. Anantram, Interbase electronic coupling for transport through DNA, *Phys. Rev. B* Vol. 71, 115405, 2005.
 - ²⁹ A.A. Voityuk, Electronic couplings and on-site energies for hole transfer in DNA: Systematic quantum mechanical/molecular dynamic study, *J. Chem. Phys.* **128** (2008) 115101.
 - ³⁰ G. Cuniberti, L. Craco, D. Porath, and C. Dekker, Backbone-induced semiconducting behavior in short DNA wires, *Phys. Rev. B* **65** (2002) 241314 (R).
 - ³¹ S. Roche, D. Bicout, E. Maciá, and E. Kats, Long Range Correlations in DNA: Scaling Properties and Charge Transfer Efficiency, *Phys. Rev. Lett.* **91** (2003) 228101.
 - ³² S. Roche, Sequence Dependent DNA-Mediated Conduction, *Phys. Rev. Lett.* **91** (2003) 108101.
 - ³³ F. Palmero, J.F.R. Archilla, D. Hennig, and F.R. Romero, Effect of base-pair inhomogeneities on charge transport along the DNA molecule, mediated by twist and radial polarons, *New J. Phys.* **6** (2004) 13.
 - ³⁴ H. Yamada, Localization of electronic states in chain models based on real DNA sequence, *Phys. Lett. A* **332** (2004) 65.
 - ³⁵ V.M. Apalkov and T. Chakraborty, Electron dynamics in a DNA molecule, *Phys. Rev. B* **71** (2005) 033102.
 - ³⁶ D.K. Klotsa, R.A. Römer, and M.S. Turner, Electronic Transport in DNA, *Biophys. J.* **89** (2005) 2187.
 - ³⁷ C.T. Shih, S. Roche, R.A. Römer, Point-Mutation Effects on Charge-Transport Properties of the Tumor-Suppressor Gene p53, *Phys. Rev. Lett.* **100** (2008) 018105.
 - ³⁸ Y.S. Joe, S.H. Lee, E.R. Hedin, Electron transport through asymmetric DNA molecules, *Phys. Lett. A* **374** (2010) 2367.
 - ³⁹ E.L. Albuquerque, U.L. Fulco, V.N. Freire, E.W.S. Caetano, M.L. Lyra, F.A.B.F. de Moura, DNA-based nanobiostructured devices: The role of quasiperiodicity and correlation effects, *Physics Reports* **535**, 139 (2014).
 - ⁴⁰ G. Cuniberti, E. Maciá, A. Rodríguez, and R.A. Römer, Chapter: Tight-Binding Modeling of Charge Migration in DNA Devices, pp. 1-20 in T. Chakraborty (editor), *Charge Migration in DNA Perspectives from Physics, Chemistry, and Biology*, 2007, Springer-Verlag Berlin Heidelberg.
 - ⁴¹ K. Lambropoulos, K. Kaklamanis, G. Georgiadis, and C. Simserides, THz and above THz electron or hole oscillations in DNA dimers and trimers, *Ann. Phys. (Berlin)* **526**, 249 (2014).
 - ⁴² K. Lambropoulos, K. Kaklamanis, G. Georgiadis, M. Theodorakou, M. Chatzieleftheriou, M. Tassi, A. Morphis and C. Simserides, THz oscillations in DNA monomers, dimers and trimers, *Proceedings of PIERS 2015 (Progress In Electromagnetics Research Symposium)*, Prague, Czech Republic, 06-09 July, 2015.
 - ⁴³ L.G.D. Hawke, G. Kalosakas, and C. Simserides, Electronic parameters for charge transfer along DNA, *Eur. Phys. J. E* **32** (2010) 291; *ibid.* Erratum to: Electronic parameters for charge transfer along DNA, **34** (2011) 118.
 - ⁴⁴ M.J.C. Gover, The eigenproblem of a tridiagonal 2-Toeplitz matrix, *Linear Algebra and its Applications* **197-198** (1994) 63.
 - ⁴⁵ Said Kouachi, Eigenvalues and eigenvectors of tridiagonal matrices, *Electronic Journal of Linear Algebra* **15** (2006) 115.
 - ⁴⁶ R. Alvarez-Nodarse, J. Petronilho, N.R. Quintero, On some tridiagonal k-Toeplitz matrices: Algebraic and analytical aspects. Applications, *Journal of Computational and Applied Mathematics* **184** (2005) 518.